NISTIR 4782

MEASUREMENT OF STRUCTURAL RESPONSE CHARACTERISTICS OF FULL-SCALE BUILDINGS: ANALYTICAL MODELING OF THE SAN BRUNO COMMERCIAL OFFICE BUILDING

Long T. Phan
Erik M. Hendrickson
Richard D. Marshall

March 1992
Building and Fire Research Laboratory
National Institute of Standards and Technology
Gaithersburg, MD 20899

U.S. Department of Commerce
Rockwell A. Schnabel, *Acting Secretary*
Technology Administration
Robert M. White, *Under Secretary for Technology*
National Institute of Standards and Technology
John W. Lyons, *Director*

PB92-171974

NIST-114A
(REV. 3-90)

U.S. DEPARTMENT OF COMMERCE
NATIONAL INSTITUTE OF STANDARDS AND TECHNOLOGY

BIBLIOGRAPHIC DATA SHEET

1. PUBLICATION OR REPORT NUMBER
NISTIR 4782

2. PERFORMING ORGANIZATION REPORT NUMBER

3. PUBLICATION DATE
MARCH 1992

4. TITLE AND SUBTITLE
Measurement of Structural Response Characteristics of Full-Scale Buildings: Analytical Modeling of the San Bruno Commercial Office

5. AUTHOR(S)
Long T. Phan, Erik M. Hendrickson, Richard D. Marshall

6. PERFORMING ORGANIZATION (IF JOINT OR OTHER THAN NIST, SEE INSTRUCTIONS)
U.S. DEPARTMENT OF COMMERCE
NATIONAL INSTITUTE OF STANDARDS AND TECHNOLOGY
GAITHERSBURG, MD 20899

7. CONTRACT/GRANT NUMBER

8. TYPE OF REPORT AND PERIOD COVERED

9. SPONSORING ORGANIZATION NAME AND COMPLETE ADDRESS (STREET, CITY, STATE, ZIP)

NIST CATEGORY #140

10. SUPPLEMENTARY NOTES

11. ABSTRACT (A 200-WORD OR LESS FACTUAL SUMMARY OF MOST SIGNIFICANT INFORMATION. IF DOCUMENT INCLUDES A SIGNIFICANT BIBLIOGRAPHY OR LITERATURE SURVEY, MENTION IT HERE.)

A 6-story commercial office building in San Bruno, California, which experienced the Loma Prieta earthquake of October 17, 1989 and sustained no visible damage, was subjected to ambient vibration tests in September 1990. Ambient vibration data were recorded from the 13 accelerometers installed prior to the Loma Prieta earthquake. Comparison of dynamic characteristics revealed that the first-mode response frequency deduced from the Loma Prieta records is significantly lower than that deduced from ambient vibration tests, and the damping ratio for strong motion is substantially higher than that obtained from ambient vibration. A computer model of the building was developed and applied using two different boundary conditions; fixed-based and spring-supported conditions. The fixed-base condition was used to simulate the building response to ambient vibration, and the spring-supported condition was used to incorporate soil-structure interaction and thus simulate realistic building response to the Loma Prieta earthquake. Results of analyses showed that the first-mode response frequencies for the two cases differ by essentially the same factor observed from measurements. This suggests that the difference in first-mode response frequencies between ambient vibration and strong motion in this building was due largely to soil-structure interaction.

12. KEY WORDS (6 TO 12 ENTRIES; ALPHABETICAL ORDER; CAPITALIZE ONLY PROPER NAMES; AND SEPARATE KEY WORDS BY SEMICOLONS)

accelerations; ambient vibration; analytical modeling; autocorrelation; buildings; damping; earthquake; Fourier spectrum; frequencies; instrumentation; Loma Prieta; measurement; modal analysis; structural response; transient analysis

13. AVAILABILITY

[X] UNLIMITED

[ ] FOR OFFICIAL DISTRIBUTION. DO NOT RELEASE TO NATIONAL TECHNICAL INFORMATION SERVICE (NTIS).

[ ] ORDER FROM SUPERINTENDENT OF DOCUMENTS, U.S. GOVERNMENT PRINTING OFFICE, WASHINGTON, DC 20402.

[X] ORDER FROM NATIONAL TECHNICAL INFORMATION SERVICE (NTIS), SPRINGFIELD, VA 22161.

14. NUMBER OF PRINTED PAGES
50

15. PRICE
A03

ELECTRONIC FORM

ABSTRACT

A 6-story commercial office building in San Bruno, California, which experienced the Loma Prieta earthquake of October 17, 1989 and sustained no visible damage, was subjected to ambient vibration tests in September 1990. Ambient vibration data were recorded from the 13 accelerometers installed prior to the Loma Prieta earthquake. Comparison of dynamic characteristics revealed that the first-mode response frequency deduced from the Loma Prieta records is significantly lower than that deduced from ambient vibration tests, and the damping ratio for strong motion is substantially higher than that obtained from ambient vibration. A computer model of the building was developed and applied using two different boundary conditions; fixed-base and spring-supported conditions. The fixed-base condition was used to simulate the building response to ambient vibration, and the spring-supported condition was used to incorporate soil-structure interaction and thus simulate realistic building response to the Loma Prieta earthquake. Results of analyses showed that the first-mode response frequencies for the two cases differ by essentially the same factor observed from measurements. This suggests that the difference in first-mode response frequencies between ambient vibration and strong motion in this building was due largely to soil-structure interaction.

Keywords: Accelerations; ambient vibration; analytical modeling; autocorrelation; buildings; damping; earthquake; Fourier spectrum; frequencies; instrumentation; Loma Prieta; measurement; modal analysis; structural response; transient analysis.

TABLE OF CONTENTS

LIST OF TABLES

LIST OF FIGURES

LIST OF FIGURES (continued)

LIST OF FIGURES (continued)

MEASUREMENT OF STRUCTURAL RESPONSE CHARACTERISTICS OF FULL-SCALE BUILDINGS: ANALYTICAL MODELING OF THE SAN BRUNO COMMERCIAL OFFICE BUILDING

1. INTRODUCTION

1.1 Background

Approximately one year after the Santa Cruz Mountains (Loma Prieta) earthquake (LPE) of October 17, 1989, an ambient vibration test program was initiated by the National Institute of Standards and Technology (NIST) in collaboration with the United States Geological Survey (USGS) to study the structural response characteristics of five existing buildings in the San Francisco Bay area. The objective of this ambient vibration test program and subsequent study is to compare the structural response characteristics of buildings obtained under ambient conditions (low-level vibration due mostly to wind) with the building response characteristics obtained from the LPE. The comparison is then used to establish minimum requirements for the dynamic measurement of structural response characteristics of full-scale buildings. The five buildings selected for this study are: (1) the California State University Administration Building at Hayward, (2) the Santa Clara County Office Building in San Jose, (3) the Commercial Office Building in San Bruno, (4) the Transamerica Building in San Francisco, and (5) the Pacific Park Plaza Building in Emeryville. These buildings represent a cross section of contemporary structural systems, materials and aspect ratios. All five buildings were instrumented prior to the LPE, the first three buildings listed above by the California Division of Mines and Geology (CDMG), and the latter two by the USGS. None of the buildings experienced visible structural damage during the LPE. Digital signal processing was performed on both the building response data recorded during the LPE and the ambient vibration data obtained from this test program. More details concerning the building descriptions and the findings and conclusions of the test program may be found in [Marshall, Phan, Celebi, February 1991 and 1992]. In general, two major differences between the building response characteristics due to ambient vibration and due to strong motion (LPE) are observed:

1. For all five buildings, the structural response frequencies determined from the LPE records (f_{LPE}) are lower than those obtained from the ambient vibration tests (f_{amb}). The first-mode frequency ratios between the LPE and the ambient vibration, f_{LPE}/f_{amb}, range between 0.68 to 0.88.

2. For all five buildings, the damping ratios computed from the LPE records, ζ_{LPE}, either by the system identification techniques [Celebi, Phan, Marshall, 1991] or by the autocorrelation techniques [Brook & Wynne, 1988; Proakis & Manolakis, 1988], are always higher than the damping ratios computed from ambient vibration recordings, ζ_{amb}. The ζ_{LPE}/ζ_{amb} ratios range between 1.0 to 19.3 for the five buildings in this test program.

The observed differences in response characteristics may be attributed, in part, to the fundamental differences in building response to ambient wind excitations and to seismic excitations. Under ambient conditions, excitation is generated largely by wind acting on the upper part of the structure and the amplitude of excitation and of structural displacement is generally small. Thus, non-structural partitions, cladding, etc. are unlikely to be mobilized and contribute to the overall structural stiffness and damping of the buildings. Further, soil-structure interaction under ambient conditions is nonexistent or at most insignificant. On the other hand, under seismic conditions, excitation is transmitted from the ground to the upper structure. Thus, soil-structure interaction is expected to influence the structural response. Further, non-structural partitions and cladding may also contribute to the overall stiffness and damping of the structure due to larger amplitude of excitations and displacements.

Of the five buildings tested in the ambient vibration test program, two are concrete structures, two are steel structures, and one is of mixed construction. It should be noted here that the most pronounced differences in the measured first-mode response frequencies, as indicated by the f_{LPE}/f_{amb} ratios, are found in the two concrete buildings, the San Bruno Commercial Office Building and Pacific Park Plaza (0.69 and 0.79, respectively). Since stiffness is proportional to the square of frequency, the ratios of stiffness as predicted by the LPE to that predicted by ambient wind excitation is 0.48 for the San Bruno Commercial Office Building and 0.62 for Pacific Park Plaza [Marshall, Phan, Celebi, 1992]. These are significant differences and call into question the appropriateness of relying on ambient vibration test results for earthquake design purposes. Thus, the cause for the observed frequency difference is the subject investigated in this report.

1.2 Objective and Scope of Report

1.2.1 Objective

This report describes the analytical modeling of the six-story, reinforced concrete, San Bruno Commercial Office Building, and the results of subsequent modal and transient dynamic analyses of the model. Specifically, the computer model was developed to provide a quantitative examination of important factors, such as the effects of an elastic foundation (soil-structure interaction) and of varying damping ratios, on the observed difference in building response frequencies as revealed by ambient wind and strong motion (LPE) response records.

1.2.2 Scope

Chapter 2 provides a detailed description of the San Bruno Commercial Office Building and a summary of existing strong-motion instrumentation. Also summarized in this chapter are the structural response characteristics of the building as obtained from the LPE and from ambient vibration tests.

Chapter 3 describes the finite element model of the building and the results of modal and transient dynamic analyses of the model. Comparisons between model responses and field-measured responses are also provided in this chapter.

Chapter 4 summarizes the overall analytical study and presents the conclusions drawn from the results of this study.

2. THE SAN BRUNO COMMERCIAL OFFICE BUILDING

The San Bruno Commercial Office Building is a 6-story, reinforced concrete moment-frame structure, located approximately 81 km northwest of the LPE's epicenter. The building is rectangular in plan, 61.26 m x 27.13 m (N-S x E-W), except that the corners have 1.4 m chamfers. The total building height is 24 m. All six floors of the building are above ground level. Figure 2.1 shows a view of this building to the southeast.

2.1 Structural System Description

There are a total of 13 east-west frames in the building. They are composed of perimeter cast-in-place spandrel beams, interior precast, post-tensioned beams, and exterior cast-in-place columns encased by precast concrete wall panels. The sixth frame from the south, 4.88 m south of the geometric center of the building, is made up of larger, more heavily reinforced cast-in-place beams and columns to provide added shear resistance to the building in the east-west direction. This arrangement provides the building with almost the same lateral stiffness in the N-S and E-W directions, despite the plan aspect ratio of more than 2 to 1. A typical floor plan is shown in Figure 2.2.

2.1.1 Columns

There are a total of 52 columns for each floor. The first-story columns are 4.27 m in height while the columns of the other stories are 3.81 m in height. The perimeter columns are cast-in-place reinforced concrete, encased by precast wall panels of irregular shape, which results in columns with composite cross sections that are roughly trapezoidal in shape. Little is known of these encasing precast wall panels and how these panels interact with the cast-in-place columns. They appear to be a proprietary design. The interior columns are reinforced concrete with square cross sections (0.51 m x 0.51 m). Typical column cross sections are shown in Figure 2.3. The perimeter columns are supported by individual spread footings which are typically 1.83 m x 3.05 m in plan and 0.91 m thick. The footings for the interior columns are square, 2.9 m x 2.9 m, and 0.91 m thick.

2.1.2 Beams

For each floor, there are a total of 34 perimeter and 20 interior beams. The perimeter beams are cast-in-place reinforced concrete with rectangular cross sections. The dimensions of the perimeter beams are 0.56 m x 0.76 m for the second floor and the roof, and 0.56 m x 0.74 m for the third to the sixth floors. Typical span for the perimeter beams is 4.88 m. The interior beams are precast, post tensioned beams with a span of 12.8 m. These beams have an I-shaped cross section and contain from 8 to 13 post-tensioning tendons. Typical beam cross sections are shown in Figure 2.4. Grade beams are similar to the spandrel beams on a typical floor.

2.1.3 Floor Slabs

The floor slabs are reinforced concrete and are 0.14 m thick, except the north and south end bays which are 0.17 m thick and the bays adjacent to these end bays which have a tapered thickness of 0.17 m to 0.14 m. The ground floor is a slab on grade and is 0.13 m thick. Offices are arranged around the perimeter of a typical floor. A steel-framed mechanical penthouse floor, 29.26 m x 10.77 m (N-S x E-W) in plan and 3.96 m in height, is located at the center of the roof. The steel frames are composed of 21 structural square tubing to support the penthouse roof. The total estimated weight of the penthouse plus mechanical equipment is 19,000 kgf. The roof slab is 0.15 m thick, except the area under the penthouse which has a thickness of 0.18 m.

2.2 Existing Strong-Motion Instrumentation

Detailed information relating to the existing strong-motion instrumentation, building response to strong motion (LPE) and ambient vibration, and the NIST data acquisition system used in ambient vibration testing may be found in [Marshall, Phan, Celebi, 1991]. Only essential information relating to the above mentioned subjects are repeated here.

The San Bruno Commercial Office Building was instrumented by CDMG as part of the California Strong Motion Instrumentation Program (CSMIP). There were a total of 13 force balance accelerometers (FBA) installed in this building at the time of the LPE. The accelerometers are distributed along the elevation of the building, at the roof, 5th floor, 2nd floor, and ground floor. The instrumentation scheme for this building is shown in Figure 2.5. Strong motion recordings were by means of auto-triggering. Strong-motion accelerations were recorded on strip film and subsequently digitized at a sampling rate of 200 Hz. Ambient vibration measurements were carried out by connecting all 13 existing accelerometers to the NIST's portable data acquisition system, and ambient vibration data were recorded with a sampling rate of 50 Hz per data channel.

2.2.1 Structural Response to Strong-Motion (LPE)

The 60-second windows of baseline-corrected and bandpass-filtered acceleration time histories and their corresponding Fourier amplitude spectra for the three roof-level accelerometers are shown in Figures 2.6 to 2.8. Of the three roof-level accelerometers, two are at the center of the roof, one in the N-S and one in the E-W direction. The remaining accelerometer is at the north end of the roof, in the E-W direction. These response data were provided by CDMG. The filter band used has ramps of 0.15-0.30 to 23.0-25.0 Hz.

In the N-S direction, a peak acceleration of 240.9 cm/sec^2 was recorded for the center of the roof 11.62 seconds after triggering. The Fourier amplitude spectrum for this location shows four spectral peaks at 0.76, 1.17, 1.37, and 1.87 Hz, respectively. The first spectral peak of 0.76 Hz has been identified as the soil system resonance frequency, and the

peak at 1.17 Hz has been identified as the first translational mode of the building in the N-S direction [Marshall, Phan, Celebi, 1992]. The damping ratio, calculated by the system identification technique for the first N-S translational mode, is 7.2 percent of critical damping.

In the E-W direction, a peak acceleration of 309.8 cm/sec^2 was recorded at the center of the roof 13.82 seconds after triggering, and a peak acceleration of 443.0 cm/sec^2 was recorded at the north end of the roof 14.3 seconds after triggering. Three spectral peaks at 0.60, 0.98, and 1.32 Hz, respectively, are identifiable on both Fourier spectra. The 0.60 Hz peak appears to be due to soil system resonance. The 0.98 Hz peak is identified as the first E-W translational mode of the building. The 1.32 Hz peak is identified as a torsional mode, as can be seen in Figure 2.9 which shows the Fourier amplitude spectra of the difference of the two EW accelerometers. The damping ratio for the first E-W translational mode is identified by the system identification technique to be 4.1 percent of critical damping [Celebi, Phan, Marshall, 1991].

In addition, normalized Fourier spectra which show the relative spectral amplitudes for accelerations at four locations along the building elevation (roof, fifth floor, second floor, and ground floor) in both the N-S and E-W directions are shown in Figure 2.10. Note that the frequencies are plotted in log scale. From the normalized E-W Fourier spectra (Figure 2.10 b), the maximum normalized spectral amplitudes were extracted for the roof, fifth floor, second floor, and ground floor (1.0, 0.822, 0.214, 0.143, respectively), and plotted with respect to the building elevation to obtain the first-mode response mode shape (E-W translation) shown in Figure 2.10 c. Note that, in Figure 2.10 c, the Fourier amplitudes were renormalized by obtaining the relative Fourier amplitudes at all four elevations with respect to that of the ground floor (thus reset the amplitude at the ground level to zero), and dividing all amplitudes by the maximum spectral amplitude at the roof.

2.2.2 Structural Response to Ambient Vibration

Ambient vibration tests on this building were performed on the morning of September 6, 1990, which was a regular work day. At the time of testing, the building was fully occupied and the building's mechanical equipment was in operation. Figures 2.11 to 2.13 show 42-second windows of baseline-corrected, low-pass filtered ambient vibration response data recorded by the same three roof-level accelerometers discussed in section 2.2.1. Also shown are the corresponding Fourier amplitude spectra. Note that the ambient vibration response data are presented in the units of microvolts.

The Fourier spectrum for the N-S direction shows a major spectral peak at 1.72 Hz. This frequency has been identified as the first translational mode frequency in the N-S direction of this building [Marshall, Phan, Celebi, 1992].

For the E-W direction, both Fourier spectra at the center and at the north end of the roof show two identifiable spectral peaks, at 1.41 and 1.95 Hz. The 1.41 Hz peak is judged to

the frequency of a torsional mode by examining the Fourier spectrum of the differences of the data of the two roof-level E-W accelerometers (see Figure 2.14).

Overall structural damping of the building was obtained from the logarithmic decrement of the ambient vibration autocorrelation function. Figures 2.15 and 2.16 show the autocorrelation function of data recorded at the center of the roof in the N-S and E-W directions, respectively. Logarithmic decrements of the autocorrelations yield damping ratios, ζ_{amb}, of 2.2 and 2.3 percent of critical in the N-S and E-W directions, respectively ($\zeta=(100/2\pi n)\ln(R_0/R_n)$, where n is the number of cycles used in the estimation, R_0 and R_n are the amplitudes of the autocorrelation function at cycle 0 and cycle n). The normalized Fourier spectra of the center of the roof, fifth floor, second floor, and the ground floor, in the N-S and E-W directions are shown in Figure 2.17. As described in section 2.2.1, the first-mode mode shape (E-W translation) due to ambient vibration was obtained from the E-W normalized Fourier spectra (Figure 2.17 b) and is plotted in Figure 2.17 c with the LPE first-mode mode shape for comparison. As can be seen from Figure 2.17 c, the displayed mode shapes due to the LPE and ambient vibration compare reasonably well.

2.3 Summary

Dynamic properties of the 6-story, reinforced concrete Commercial Office Building in San Bruno, California, obtained from the LPE records and from ambient vibration measurements are summarized below in Table 2.1. The last column in Table 2.1 shows the first-mode frequency ratios (LPE/ambient vibration). It is noted that the measured dynamic properties of this building are consistent with the general trends observed by others [Ellis and Littler, 1988; Bertero et al., 1988; Bendimerad et al., 1991], i.e. response frequency decreases with increasing displacement amplitude and damping increases with increasing displacement amplitude.

TABLE 2.1 SUMMARY OF FIRST-MODE RESPONSE OF THE BUILDING

Mode Description	Loma Prieta Earthquake		Ambient Vibration		Frequency Ratio
	f_{LPE} (Hz)	ζ_{LPE} [1] (%)	f_{amb} (Hz)	ζ_{amb} [2] (%)	(f_{LPE}/f_{amb})
EW First Translational Mode	0.98	4.1	1.41	2.3	0.70
NS First Translational Mode	1.17	7.2	1.72	2.2	0.68

[1] Obtained by system identification technique.

[2] Obtained by logarithmic decrement of auto-correlation function.

3. COMPUTER MODEL OF THE SAN BRUNO OFFICE BUILDING

A finite element model of the San Bruno Commercial Office Building was developed to study the building's structural response to the LPE and to ambient wind excitation measured in this test program. More specifically, the model was used to investigate the possible effects of soil-structure interaction and large amplitude excitation as reasons for the observed reduction in the building's fundamental response frequencies with strong motion. The computer model was created by discretizing all structural components into finite elements, interconnected at corner or end nodes to form the three-dimensional geometry. A total of 484 nodes, 837 beam and column bar elements, and 336 plate elements were used in the model. The Finite Element Analyses module of computer program Patran (P/FEA) was used in modeling and analyses. More information concerning the finite elements supported by P/FEA and used in modeling this building, and the solution procedures employed in analyzing the model may be found in [Patran P/FEA User Manual, 1989]

3.1 Modeling of Structural Systems

Columns and Beams which have finite cross-sectional dimensions were modeled using the linear two-noded bar element with six degrees-of-freedom at each end node (three translations and three rotations). Column section properties, including cross-sectional area and moments of inertia with respect to the major and minor axes, were calculated using transformed, uncracked sections. There are 13 different column cross sections in the model. The input material properties include a concrete modulus of elasticity of 28,090 MPa, based on a designed compressive strength of 34.47 MPa.

For the perimeter columns encased by the proprietary precast wall panels, it was decided that only the cast-in-place portion of the columns would be used in computing the moments of inertia. This was because little is known about the properties of the encasing precast wall panels and how they interact with the cast-in-place portion of the perimeter columns. However, it should be noted here that if, in reality, the encasing panels were effectively connected to and performed integrally with the cast-in-place columns, then the overall stiffness of the building would be underestimated by the computer model.

For the perimeter cast-in-place and the interior post-tensioned beams, transformed and uncracked section properties were also used. The majority of post-tensioned beams have 10, 11, or 12 tendons. The transformed section properties of the beams with 11 tendons were calculated and used as section properties for all post-tensioned beams. For the cast-in-place beams, a total of 4 different sets of section properties were used.

Floor and roof slabs were modeled using 4-noded quadrilateral and 3-noded triangular plate bending elements. There are 6 degrees of freedom per corner node. The only property needed to describe the plate elements was thickness. Actual slab thickness was used for the plate elements to accurately represent the stiffness, and modified mass densities were

used for these elements to account for the floor and roof loads. The plate elements which represent the tapered slabs were assigned an equivalent uniform thickness of 0.16 m, equal to the average of the thicknesses at the two ends, 0.17 m and 0.15 m.

The penthouse, which is supported by 21 square structural steel tubes, was modeled as 22 added masses located at the bases of the penthouse columns on the building roof (one of the penthouse columns did not fall on a node point, but rather, between two nodes above the shear frame - equal masses were assigned to all four nodes in this column line). The total estimated mass of the penthouse, including the penthouse roof, supporting steel beams and columns, and mechanical equipment, is 19,000 kgf. This mass was divided into 22 added masses, 18 added masses of 907 kgf each and 4 added masses of 680 kgf each. Modeling the penthouse floor as added masses does not adversely affect the accuracy of the model since the penthouse floor contributes little to the global stiffness of the structure.

3.2 Analyses of Computer Model

The computer model of the San Bruno Commercial Office building was subjected to modal and transient dynamic analyses. Modal analyses were performed to compute the natural frequencies and associated mode shapes of the model. Transient dynamic analyses were performed to obtain the dynamic response, in terms of displacement, velocity, and acceleration, of the model when subjected to known acceleration time histories. For both types of analyses, it is necessary to place an artificially large mass at the geometric center of the building at ground level. The large mass is linked to the model at the base of each column by rigid link elements. These rigid link elements are beam elements with infinite stiffness and are used to transmit motion resulting from the application of acceleration time histories at the large mass to the upper structure. The large mass selected for these analyses was given a value of several orders of magnitude greater than the total structure mass. The magnitude of the artificial mass was selected so that the response accelerations calculated for column bases would not differ significantly from the acceleration record used to drive the large mass. An idealized model with large mass and rigid links is shown in Figure 3.1. The results of modal and transient dynamic analyses are discussed below.

3.2.1 Modal Analyses

Modal analyses were performed on the model with two different sets of boundary conditions; fixed-base and spring-supported conditions. For the fixed-base model, the base columns were connected to the large mass directly using the rigid link elements. Since the rigid link elements are infinitely stiff, the ends of the columns which are connected to the rigid links are considered fixed. This boundary condition is thought to simulate best the ambient vibration condition since soil-structure interaction is completely ignored. For the spring-supported model, a set of discrete, two-noded spring elements consisting of one vertical and two horizontal springs with finite lengths and stiffnesses were created at the base of each column. The vertical spring elements were given a finite extensional stiffness to model the modulus of subgrade reaction. The NS and EW lateral spring elements were

given both extentional and rotational stiffnesses to model the lateral and rotational stiffnesses of the San Bruno Building at the foundation level. It is thought that, when the extensional stiffness of the vertical springs is selected to equal the soil stiffness and the horizontal spring stiffnesses are selected to equal the lateral stiffness of the building, the model will best represent the real building under earthquake excitation since soil-structure interaction is included.

3.2.1.1 Fixed-Base Model

The first five natural frequencies obtained from modal analyses of the fixed-base model are shown in Table 3.1. The associated mode shapes are plotted in Figure 3.2. The first mode frequency of 1.217 Hz is identified as the EW translational mode. The second mode of 1.283 Hz is NS translation. The third, 1.599 Hz, is a torsional mode. The fourth and fifth modes of 3.74 Hz and 3.99 Hz are EW and NS translational modes combined with floor twisting.

TABLE 3.1 NATURAL FREQUENCIES OF THE FIXED-BASE MODEL

Mode No.	Natural Frequencies (Hz)	Mode description
1	1.217	EW Translation
2	1.283	NS Translation
3	1.599	Torsion
4	3.740	EW Translation with Floor Twisting
5	3.990	NS Translation with Floor Twisting

The modal analysis results with fixed-base condition may be compared to the results for the ambient vibration tests listed in Table 2.1. It is observed that the analytically obtained natural frequencies, on average, are approximately 25 percent lower than those obtained from ambient vibration testing. Refinement of the model to include the stiffnesses of the precast wall panels, which were ignored in the current model for example, would certainly result in better agreement between the predicted and the measured response frequencies. However, since the purpose of this study is to identify the possible cause (or causes) of the reduction in response frequencies due to strong motion (LPE), no refinement of the model was attempted. Instead, the same model, only with different boundary conditions (spring-supported model), was developed to model the San Bruno Building under strong motion.

3.2.1.2 Spring-Supported Model

The spring-supported model was used to simulate the effects of soil-structure interaction. The results of this model are to be compared with those of the fixed-base model to allow an assessment of the effect of soil-structure interaction on the response frequencies. There are 52 vertical springs with finite extensional stiffnesses to represent the modulus of subgrade reaction, and 104 horizontal springs (52 NS springs and 52 EW springs) with finite extensional and rotational stiffnesses to represent the lateral and rotational stiffnesses of the building at the foundation level.

For the vertical springs, the average load per footing, computed using the estimated total structure weight of 9,278 tons and a total of 48 footings, is 193 tons. By estimating an average maximum subgrade settlement of approximately 4.2 mm for the type of soil at the San Bruno Building site, the soil stiffness, or the extensional stiffness of each vertical spring, can be approximated as 447,997 kN/m (193,000 kgf/4.2 mm equals 45,714 kgf/mm) [Bowles, 1977].

For the horizontal springs, the total lateral stiffness at the first floor level was computed using a concrete elastic modulus E_c of 28,090 MPa and a column height of 4.3 m to be approximately 3.038×10^6 kN/m in the NS direction and 3.002×10^6 kN/m in the EW direction ($k = 12EI/L^3$). From the total building stiffness, the extensional stiffness of each NS horizontal spring was computed to be 63,292 kN/m, and the extensional stiffness of each EW horizontal spring was computed to be 62,542 kN/m. It should be noted again here that only the monolithic concrete cores of the perimeter columns were considered in modeling these columns, i.e. only the properties of the monolithic cores were used in computing the cross-sectional properties. The precast wall panels that encased these columns were not modeled. Thus, if the wall panels acted integrally with the monolithic concrete cores under all load levels, then the total building lateral stiffness computed for the model and given above would be smaller than the actual stiffness of the building.

Because of many uncertainties involving the estimation of the rotational stiffnesses of the columns with individual spread footings, five different rotational spring stiffnesses, ranging from an unrealistically low value of 10^3 kN-m/radian to a high value of 10^8 kN-m/radian, were selected for modal analyses of the spring-supported model. The results of modal analyses of the spring-supported model are shown in Table 3.2.

It may be observed, from the response frequencies in Table 3.2, that varying the rotational stiffnesses of the individual spread footings, even by a factor of 10^5, results in a change of only approximately 3% in the first mode response frequency of the spring-supported model. Thus, even though a precise value of rotational stiffness could not be computed for the model due to many uncertainties, its effect on the model response frequency is insignificant. However, the effect of the modulus of subgrade reaction on the

TABLE 3.2 NATURAL FREQUENCIES OF THE SPRING-SUPPORTED MODEL

Mode No.	Rotational Stiffnesses (kN-m/rad) $1x10^8$	$1x10^7$	$1x10^6$	$0.5x10^6$	$1x10^3$	Mode Description
1	0.895	0.873	0.871	0.871	0.870	EW Translation
2	0.932	0.910	0.908	0.908	0.908	NS Translation
3	1.153	1.131	1.129	1.129	1.129	Torsion
4	3.064	3.035	3.032	3.032	3.032	EW Bending/Floor Twisting
5	3.238	3.211	3.210	3.208	3.208	NS Bending/Floor Twisting

response frequency appears to be pronounced, as can be seen by comparing the results in Table 3.2 with the results of the fixed-base model listed in Table 3.1. Assuming a rotational stiffness of 10^3 kN-m/rad for the base columns, the first mode (EW translation) frequency ratio between the spring-supported condition and the fixed-base condition, f_s/f_f, is 0.72 (0.870/1.217). For the second mode (NS translation), this frequency ratio is 0.71 (0.908/1.283). These analytically obtained frequency ratios, based on the spring-supported and fixed-base boundary conditions, f_s/f_f, can be compared with the measured frequency ratios between the LPE and the ambient vibration, f_{LPE}/f_{amb}, listed in Table 2.1. From Table 2.1, the first mode (EW translation) f_{LPE}/f_{amb} ratio is 0.70 which is approximately 3% different from the first mode f_s/f_f ratio (0.72), and the second mode (NS translation) f_{LPE}/f_{amb} ratio is 0.68 which is approximately 4% different from the second mode f_s/f_f ratio (0.71). The good agreement between the measured and analytical frequency ratios indicates that, for this particular building, the observed reduction in frequency between ambient vibration and strong motion may be attributed in large part to the effect of soil-structure interaction.

It should be noted, however, that while the observed frequency reduction in the San Bruno Commercial Office Building may be explained by accounting for the effect of soil-structure interaction using realistic values of modulus of subgrade reaction, soil-structure interaction might not be the only factor that influences this change in response frequency. It is likely that other factors, including the possibility of slip between the encasing precast wall panels and the monolithic core of the exterior columns, joint slip at the precast floor beams, and microcracking of concrete, may also have contributed in part to the observed frequency reduction. These nonlinear factors are difficult to model given the lack of knowledge of precisely how all structural components in the building interacted during the LPE and ambient vibration testing, and therefore are ignored in this study.

3.2.2 Transient Dynamic Analyses

Transient dynamic analyses using modal formulation (mode superposition) were performed on the fixed-base and the spring-supported models to compute the model responses to input acceleration time histories. Specifically, these analyses were performed to (1) study the sensitivity of the first-mode response frequency to changes in overall structural damping, (2) study the sensitivity of the first-mode response frequency to different assumptions for the value of rotational stiffness, and (3) obtain a first-mode mode shape for comparison to those previously shown for the actual building. In this study, the San Bruno model was excited using the EW component of acceleration recorded at the center of the ground floor during the LPE. The acceleration record was digitized at 0.02-second intervals and applied to the large mass to simulate ground motion. The typical record length used for transient analysis was 33 seconds. The first five modes obtained from modal analyses of the model were used for mode superposition. Contributions of modes higher than the first five structural modes to transient response of this building are judged insignificant and, therefore, are not considered.

3.2.2.1 Fixed-Base Model

Four different damping ratios, ranging from 0.5 percent to 10.0 percent of critical damping (0.5, 3.0, 7.0, and 10.0 percent), were used in the transient dynamic analyses of the fixed-base model. Figures 3.3 to 3.10 show the EW structural responses, in terms of acceleration-time histories, of the nodes located at the center of the roof and at the center of the north end of the roof. Also shown are the corresponding Fourier spectra. The model first-mode frequencies corresponding to different damping ratios were determined from the half-power bandwidth method and are summarized in Table 3.3.

TABLE 3.3 FIRST MODE FREQUENCY WITH VARYING DAMPING RATIOS FIXED-BASE MODEL

	Damping Ratios (% of Critical)			
	10.0	7.0	3.0	0.5
First Mode Frequencies (Hz)	1.212	1.216	1.227	1.235

The response acceleration-time histories at the center of the roof and at the center of the north edge of the roof compare well with the building responses recorded during the LPE (Figures 2.7 and 2.8). For each of the four different damping ratios, the elapsed time to maximum acceleration at the center of the roof is between 13 and 14 seconds, which

compares well with 13.82 seconds observed in the LPE (section 2.2.1). At the center of the north end of the roof, the elapsed time ranges from 14 to 15 seconds which compares well with the observed 14.3 seconds for the LPE. Furthermore, the peak accelerations at the north edge of the roof are higher than those at the center of the roof; similar to the response of the San Bruno Building for the LPE (section 2.2.1). This demonstrates the ability of the model to simulate the three-dimensional behavior, i.e. the torsional response, of the San Bruno Building. Moreover, from the Fourier spectra, it is apparent that damping ratios have little effect on the first mode response frequency (1.235 Hz with 0.5 percent damping vs. 1.212 Hz with 10 percent damping, or a difference in response frequency of approximately 2%).

3.2.2.2 Spring-Supported Model

As discussed in section 3.2.1.2, soil-structure interaction was examined using the spring-supported model. The results of modal analyses of the five cases listed in Table 3.2, where the rotational spring constants were varied between 10^3 to 10^8 kN-m/radian, were utilized in the modal superposition process for transient analyses. An overall damping ratio of 7 percent of critical was used in all five cases. The resulting first mode response frequencies corresponding to the five cases are listed in Table 3.4. The response acceleration time histories and corresponding Fourier spectra of the five cases are shown in Figures 3.11 to 3.15. As can be seen from Table 3.4, different assumptions for the rotational stiffness of the building at the ground level appear to have little effect on the first-mode response frequency of this building. In addition, the analytical first-mode response mode shape (EW translation) was obtained by normalizing the Fourier spectra of four nodes located at the center of the roof, fifth floor, second floor, and ground floor. These four nodes correspond to the locations of four existing accelerometers in the San Bruno Building from which measured response records were used to plot the mode shapes in Figures 2.10 c and 2.17 c. Figure 3.16 shows the first-mode response mode shapes obtained from the LPE, ambient vibration, and the spring-supported model with a rotational stiffness of 10^3 kN-m/radian and a damping ratio of 7.0 percent. As can be seen on Figure 3.16, the analytically obtained first-mode response mode shape agrees well with those mode shapes obtained from the LPE and from ambient vibration testing.

TABLE 3.4 FIRST MODE FREQUENCY WITH VARYING ROTATIONAL STIFFNESS

	Rotational Stiffnesses (kN-m/rad)				
	$1x10^8$	$1x10^7$	$1x10^6$	$0.5x10^6$	$1x10^3$
First Mode Frequencies (Hz)	0.893	0.873	0.869	0.869	0.867

4. SUMMARY AND CONCLUSIONS

4.1 Summary

Ambient vibration testing was performed on the San Bruno Commercial Office Building approximately one year after the Loma Prieta earthquake. The measured responses of the building to the LPE and to ambient vibrations are presented and compared in this report. The comparisons show reasonable agreement between the first-mode response mode shapes obtained from strong motion and from ambient vibration records. There is a significant difference in the first and second mode response frequencies of this building. The measured frequency ratio, f_{LPE}/f_{amb}, is 0.70 for the first mode response (EW translation), and is 0.68 for the second mode response (NS translation). Damping estimates deduced from ambient vibration response records by conventional auto-correlation techniques are always smaller than those deduced from the LPE response records by system identification techniques (the ζ_{LPE}/ζ_{amb} ratios range between 1.0 to 19.3).

A three-dimensional finite element model of the building was developed based on the structural drawings. The model was analyzed using two sets of boundary conditions; fixed-base and spring-supported conditions. The fixed-base model was used to predict building response to ambient vibration. The spring-supported model, where elastic behavior of the subgrade is accounted for by using a realistic value for the spring stiffness, was used to predict building response to the LPE. Subsequent modal analyses showed that the models underestimated the measured response frequencies of the building by approximately 25 percent. This difference may be attributed to several factors, one of which is the exclusion of the precast wall panels that formed the exterior columns. Better agreement might be obtained with refinement of the model to include these precast panels. However, since the interest here is in the relative difference in response frequency between the LPE and ambient vibration, refinement of the model was not performed. Comparisons between the response frequencies of the fixed-base and the spring-supported models indicate an analytical frequency ratio equal to the observed frequency ratio obtained from measurements. Further, transient dynamic analysis of the models with varying damping ratios and rotational stiffnesses indicates that these factors have little effect on the response frequency of the building. Thus, based on these results, it is concluded that, for this particular building, the frequency difference resulting from ambient wind excitation and from strong motion earthquake excitation is due mainly to soil-structure interaction.

4.2 Conclusions

The following conclusions are drawn from the current study:

- For this particular building, soil-structure interaction appears to be the primary reason for the frequency difference observed when results from ambient vibration and the LPE are compared.

- Damping ratios within the range of 0.5 to 10.0 percent have little effect on the response frequencies of the building.

- The linear elastic computer model of the San Bruno Commercial Office Building was developed primarily to study the relative effects of various assumptions and factors affecting the dynamic response of the building, and in this sense the model was successful. However, the model did not include elements to represent the precast panels which encased the exterior columns. This appears to have resulted in lower stiffness in the model than in the real building, which in turn results in a difference of approximately 25 percent in modal frequencies. This serves to illustrate that careful attention must be paid to specific details of the building in the modeling process to obtain the required accuracy if the interest is in the absolute values of the dynamic properties of the building.

5. REFERENCES

Bertero, V.V., Bendimerad, F.M., Shah, H.C., "Fundamental Period of Reinforced Concrete Moment-Resisting Frame Structures," Report No. 87, the John A. Blume Earthquake Engineering Center, Department of Civil Engineering, Standford University, October 1988.

Bendimerad, F.M., Shah, H.C., Hoskins, T., "Extension of Study on Fundamental Period of Reinforced Concrete Moment-Resisting Frame Structures," Report No. 96, the John A. Blume Earthquake Engineering Center, Department of Civil Engineering, Standford University, June 1991.

Bowles, J.E., "Foundation Analysis and Design," Second Edition, McGraw-Hill Book Company, 1977.

Brook, D., Wynne, R.J., "Signal Processing: Principles and Applications", Edward Arnold, 1988.

Celebi, M., Phan, L.T., Marshall, R.D., "Comparison of Responses of a Select Number of Buildings to the 10/17/1989 Loma Prieta (California) Earthquake and Low-Level Amplitude Test Results," NIST SP 820, Proceedings of the 23RD Joint Meeting of the U.S.-Japan Coorperative Program in Natural Resources Panel on Wind and Seismic Effects, p. 475-499, September 1991.

Ellis, B.R., Littler, J.D., "Dynamic Response of Nine Similar Tower Blocks", Journal of Wind Engineering and Industrial Aerodynamics, 28, 1988, p.p. 339-349, Elsevier Science Publishers B.V., Amsterdam, the Netherlands.

Marshall, R.D., Phan, L.T., Celebi, M., "Measurement of Structural Response Characteristics of Full-Scale Buildings: Selection of Structures", NISTIR-4511, National Institute of Standards and Technology, February, 1991.

Marshall, R.D., Phan, L.T., Celebi, M., "Measurement of Structural Response Characteristics of Full-Scale Buildings: Comparison of Results from Strong-Motion and Ambient Vibration Records", NISTIR92-xxxx, National Institute of Standards and Technology, 1992.

PDA Engineering, Patran Division, "Patran P/FEA User Manual", 2975 Redhill Avenue, Costa Mesa, California 92626, September 1989.

Proakis, J.G., Manolakis, D.G., "Introduction to Digital Signal Processing", Macmillan Publishing Company, 866 Third Avenue, New York, New York 10022, 1988.

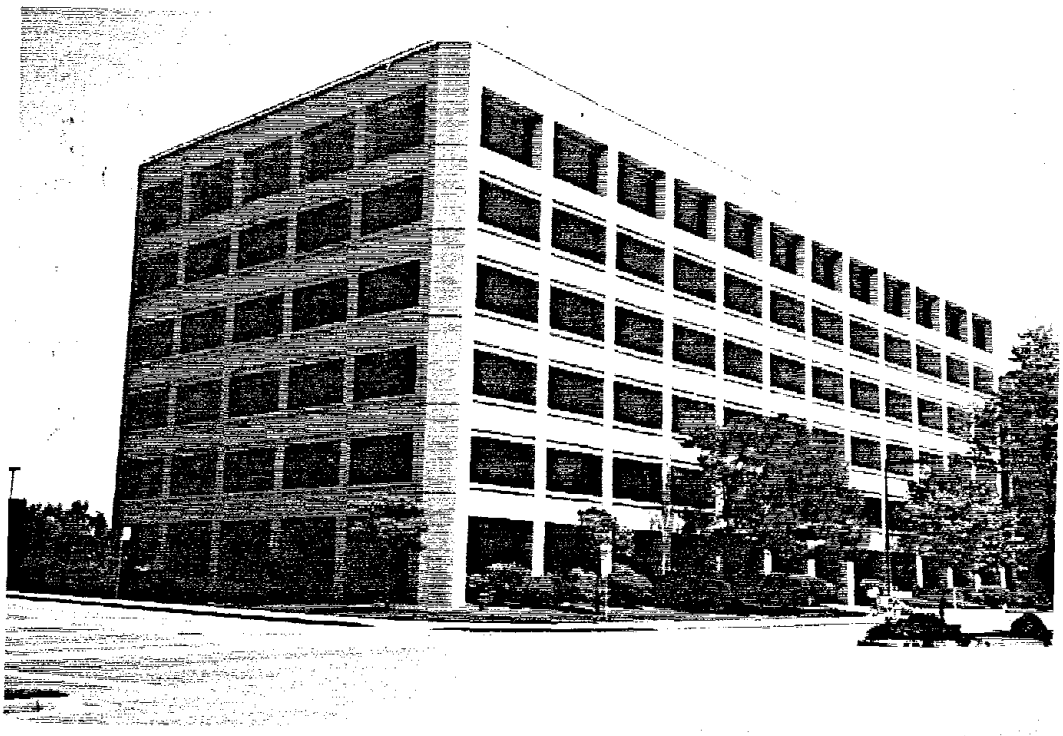

Figure 2.1 View to the Southeast of the San Bruno Commercial Office Building.

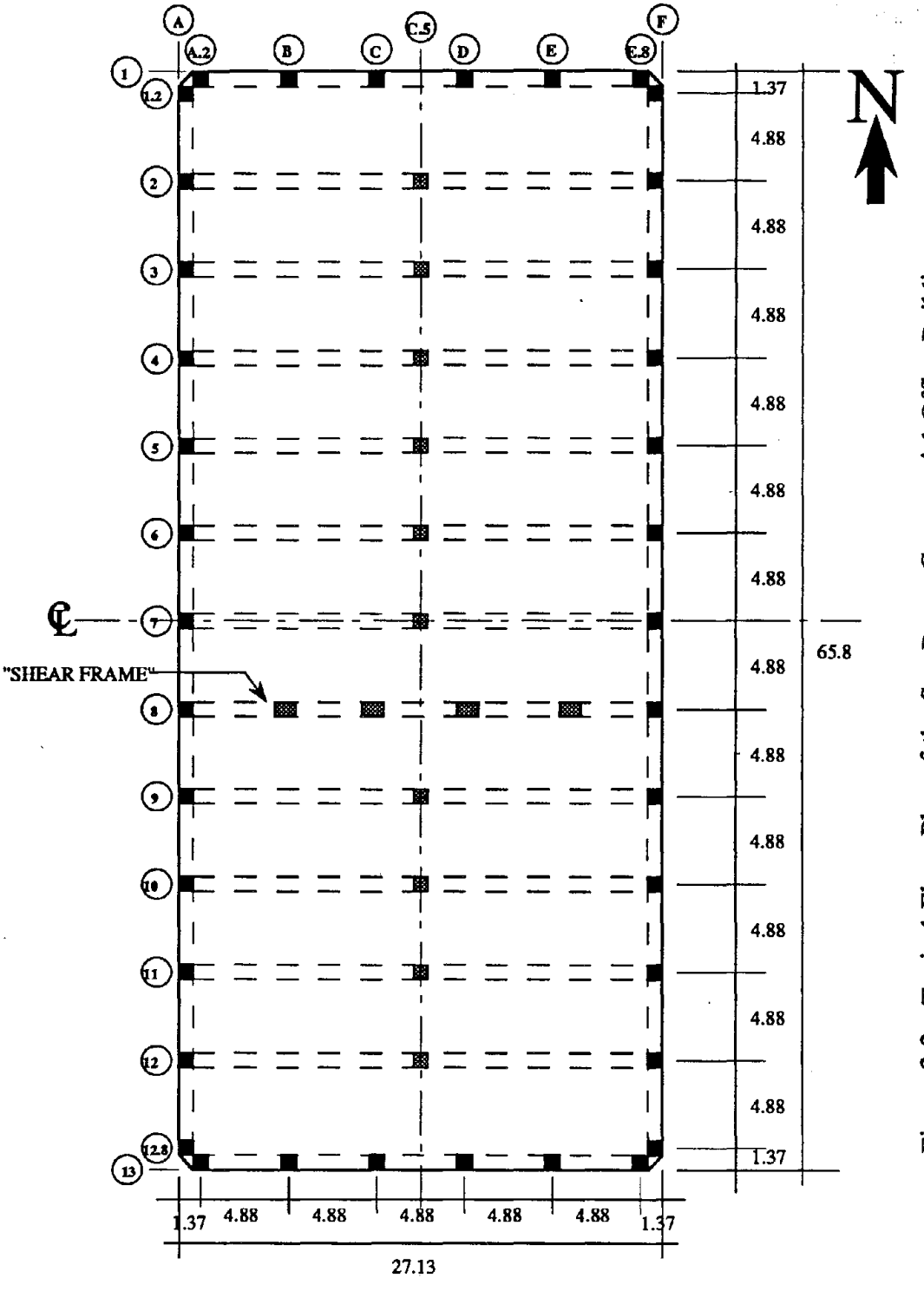

Figure 2.2 Typical Floor Plan of the San Bruno Commercial Office Building.

All Dimensions in meters

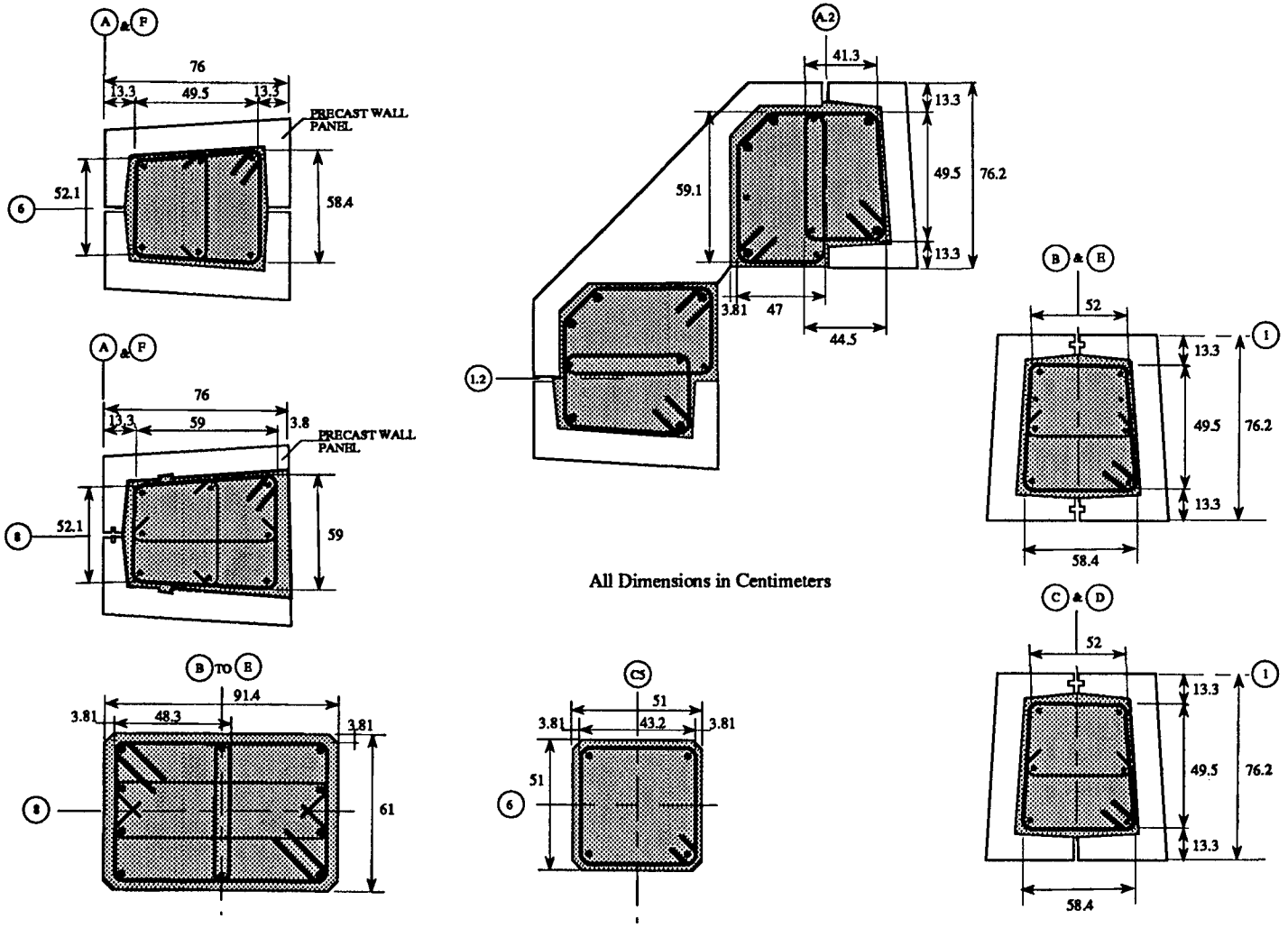

Figure 2.3 Typical Column Cross Sections.

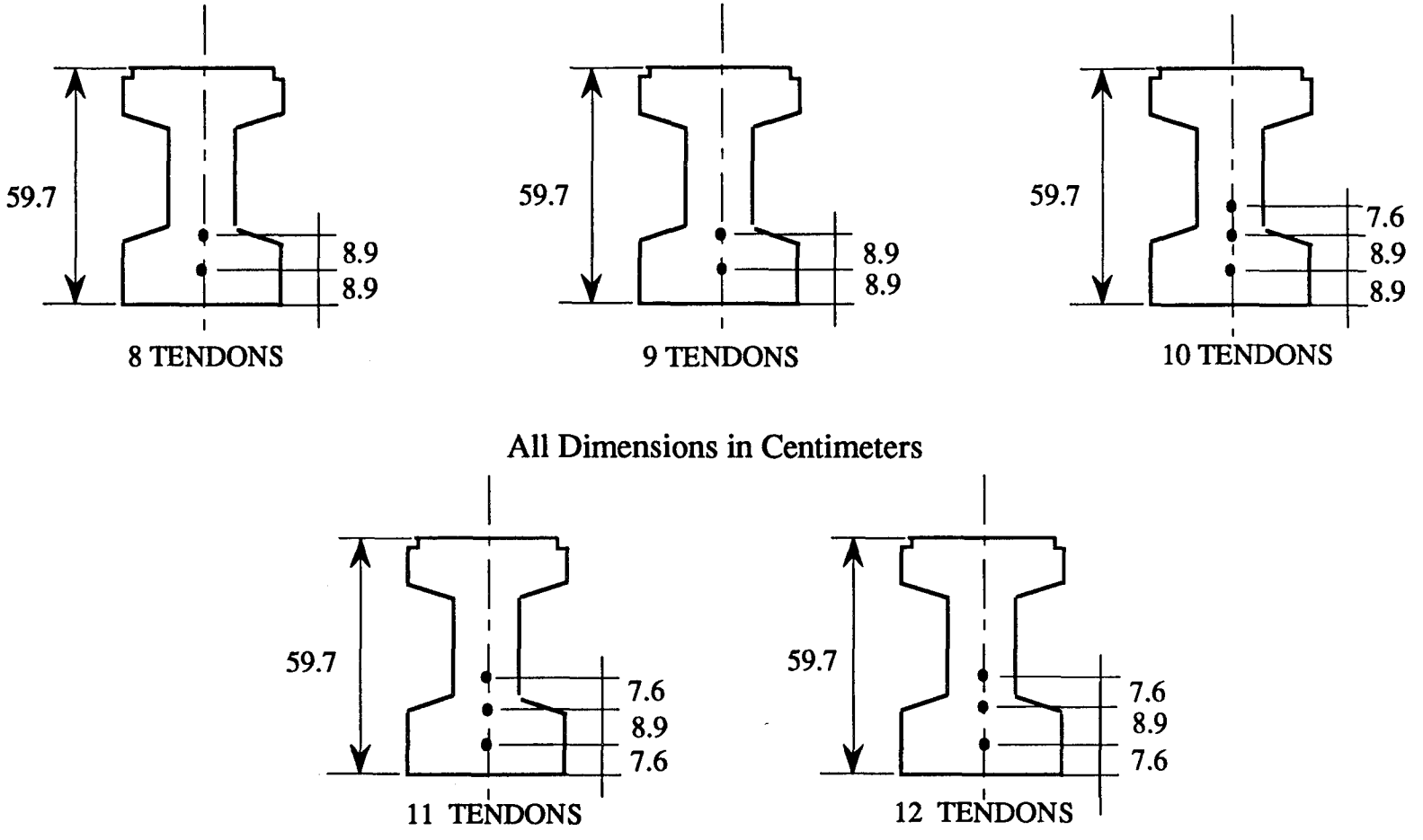

Figure 2.4 Typical Beam Cross Sections.

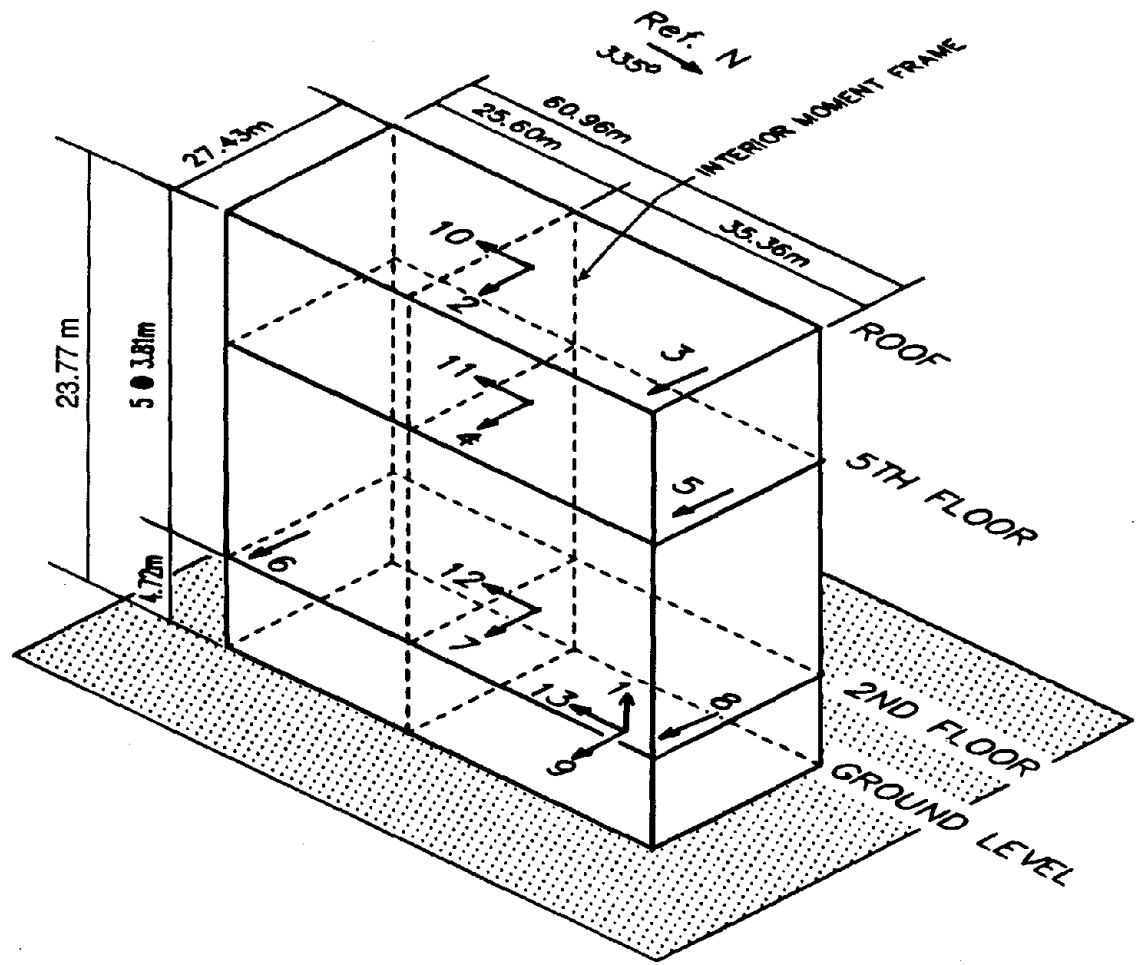

Figure 2.5 Existing Instrumentation Scheme in the San Bruno Commercial Office Building.

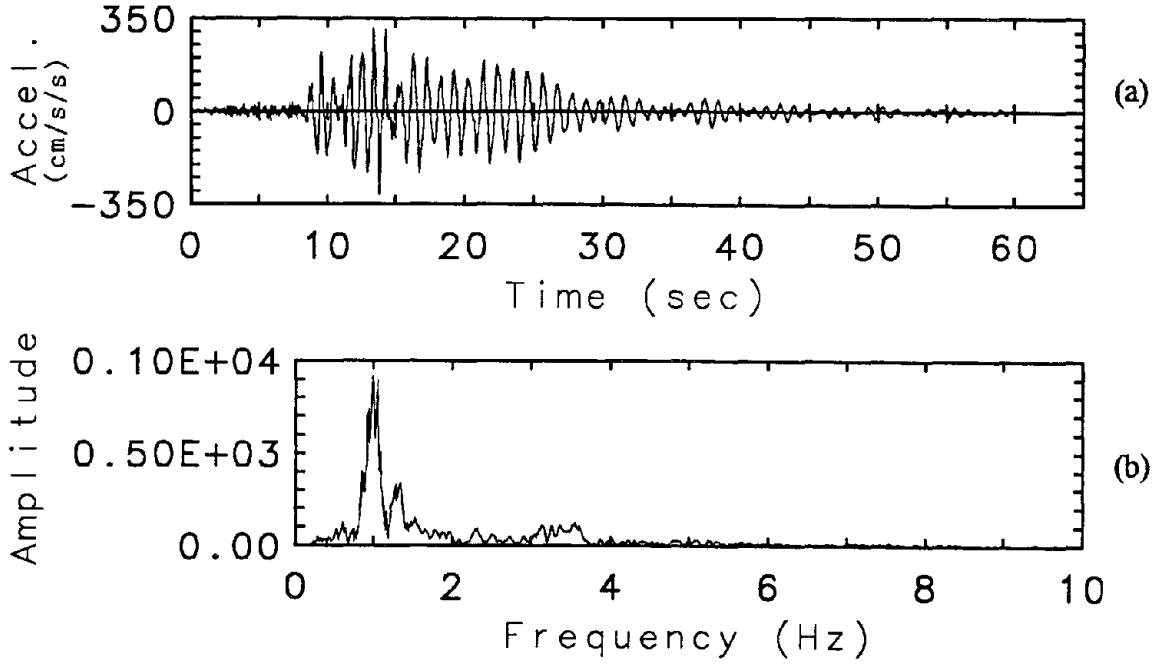

Figure 2.6 Acceleration-Time History at Center of Roof in EW Direction Due to the Loma Prieta Earthquake (a) and Corresponding Fourier Spectrum (b).

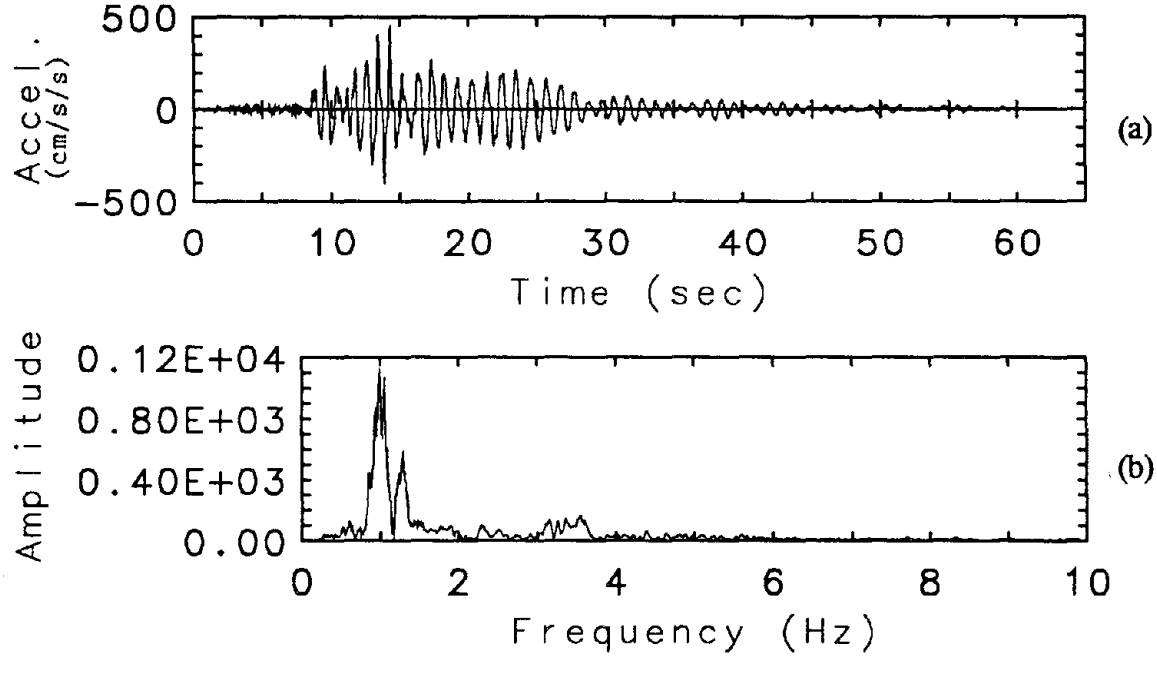

Figure 2.7 Acceleration-Time History at North end of Roof in EW Direction Due to the Loma Prieta Earthquake (a) and Corresponding Fourier Spectrum (b).

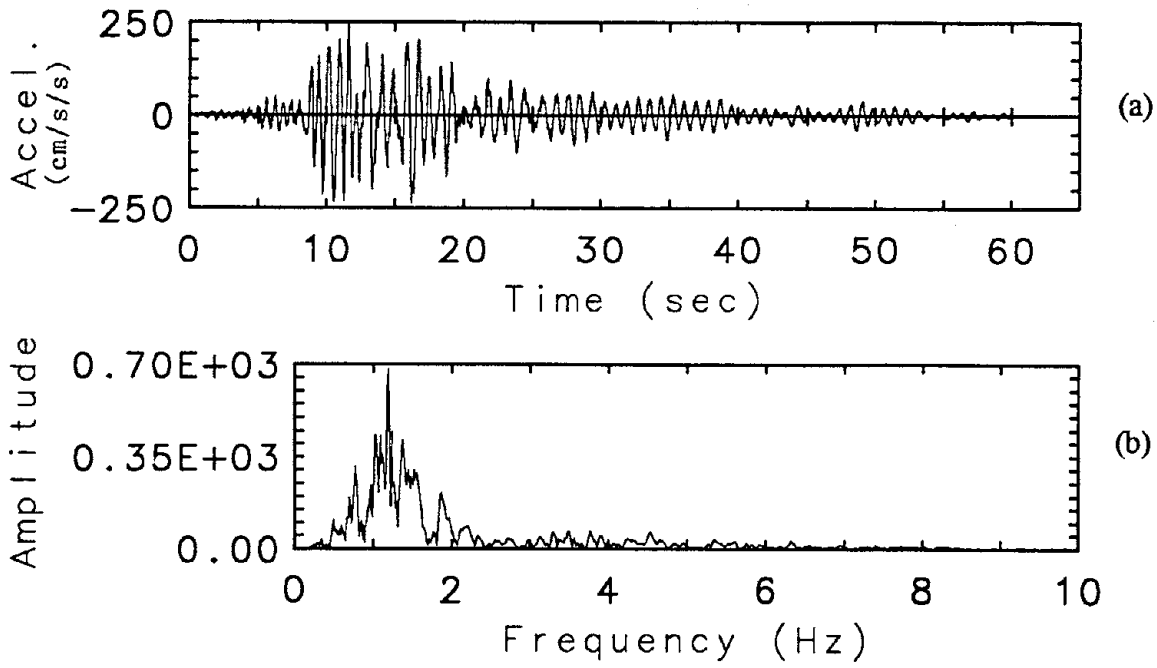

Figure 2.8 Acceleration-Time History at Center of Roof in NS Direction Due to the Loma Prieta Earthquake (a) and Corresponding Fourier Spectrum (b).

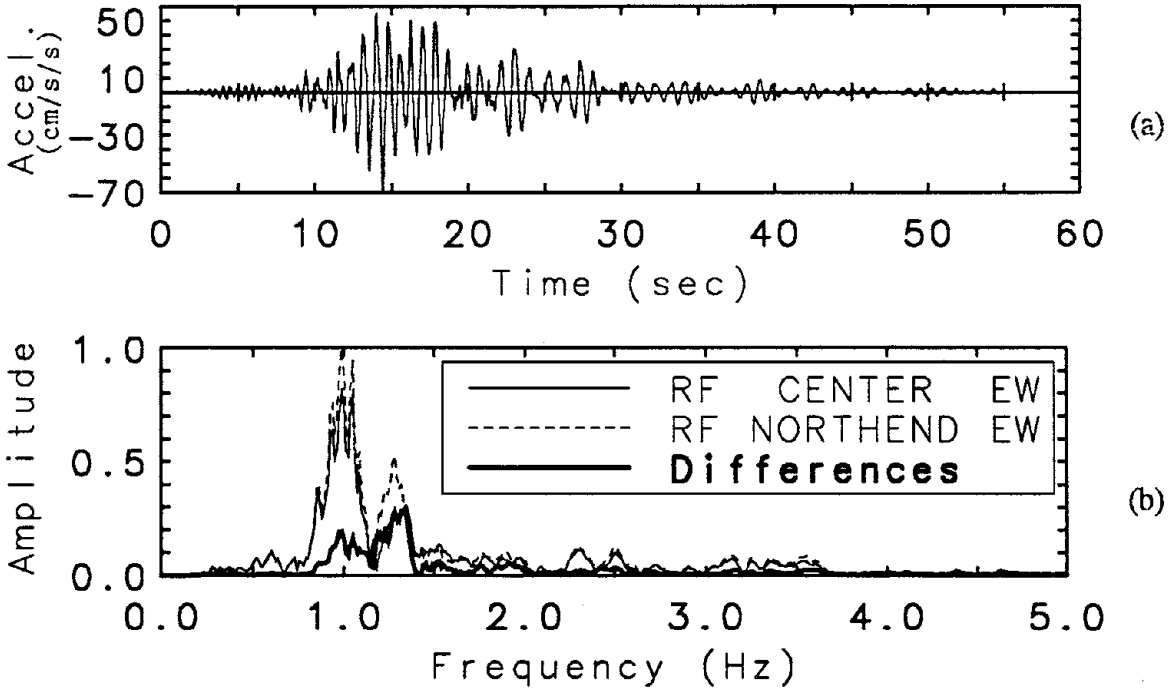

Figure 2.9 Difference of Roof-level EW Acceleration (a) and Corresponding Fourier Spectrum (b).

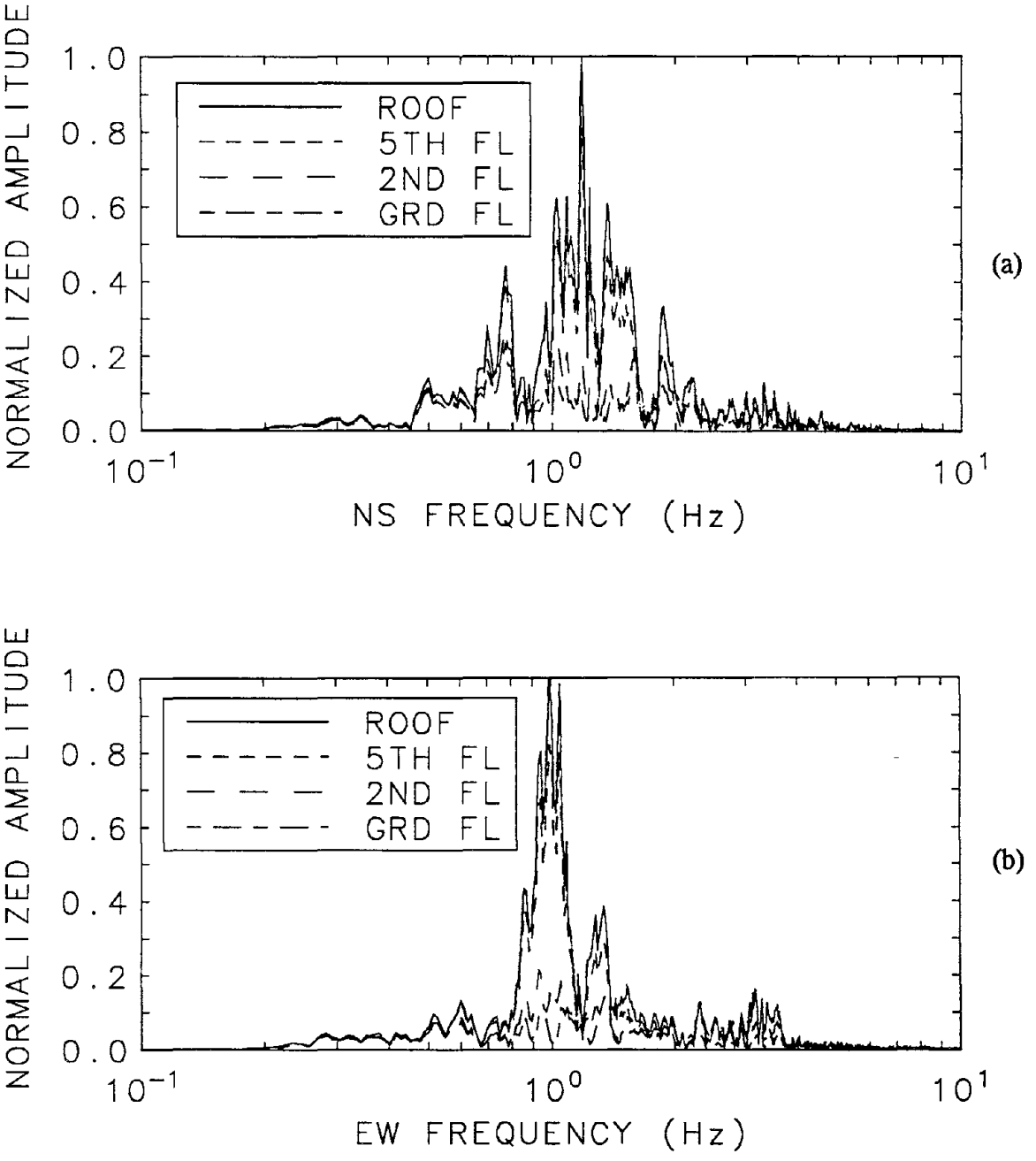

Figure 2.10 Normalized Fourier Spectra of Strong-motion Response Records at Different Elevation in NS (a), and EW (b) Directions, First-Mode Response Mode Shape due to the Loma Prieta Earthquake (c).

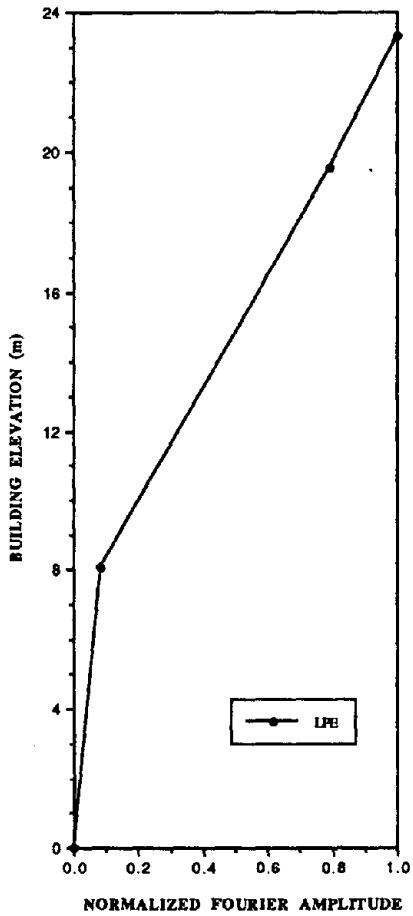

(c)

Figure 2.10 (continued)

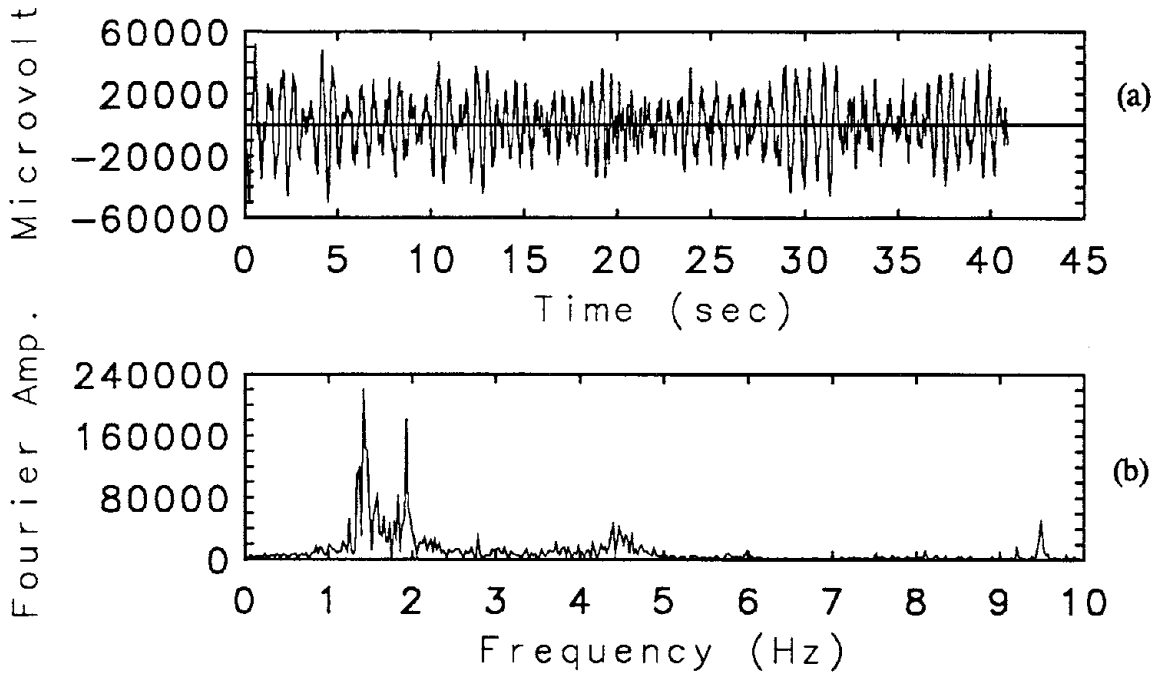

Figure 2.11 Response Time History at Center of Roof in EW Direction Due to Ambient Vibration (a) and Corresponding Fourier Spectrum (b).

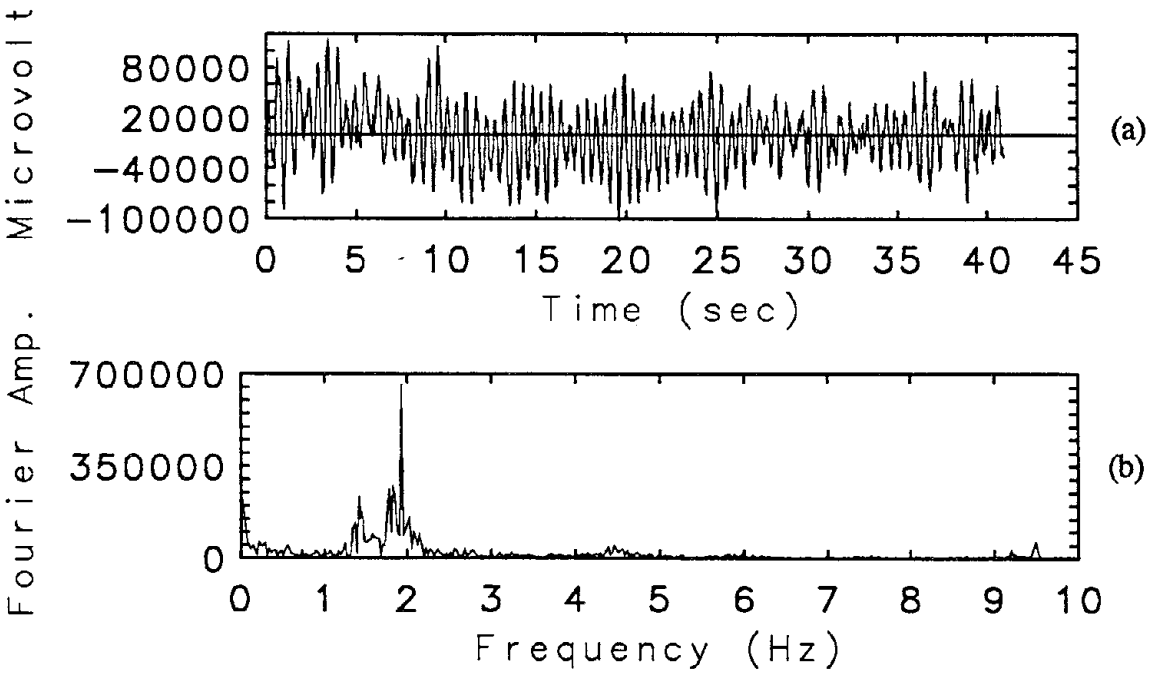

Figure 2.12 Response Time History at North end of Roof in EW Direction Due to Ambient Vibration (a) and Corresponding Fourier Spectrum (b).

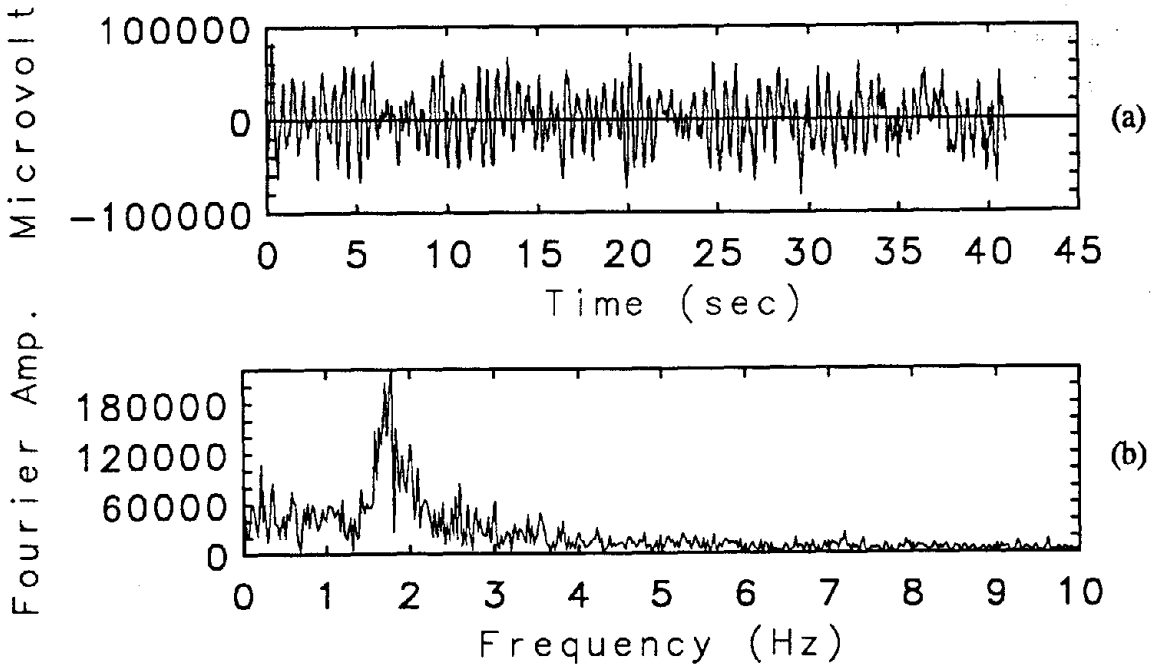

Figure 2.13 Response Time History at Center of Roof in NS Direction Due to Ambient Vibration (a) and Corresponding Fourier Spectrum (b).

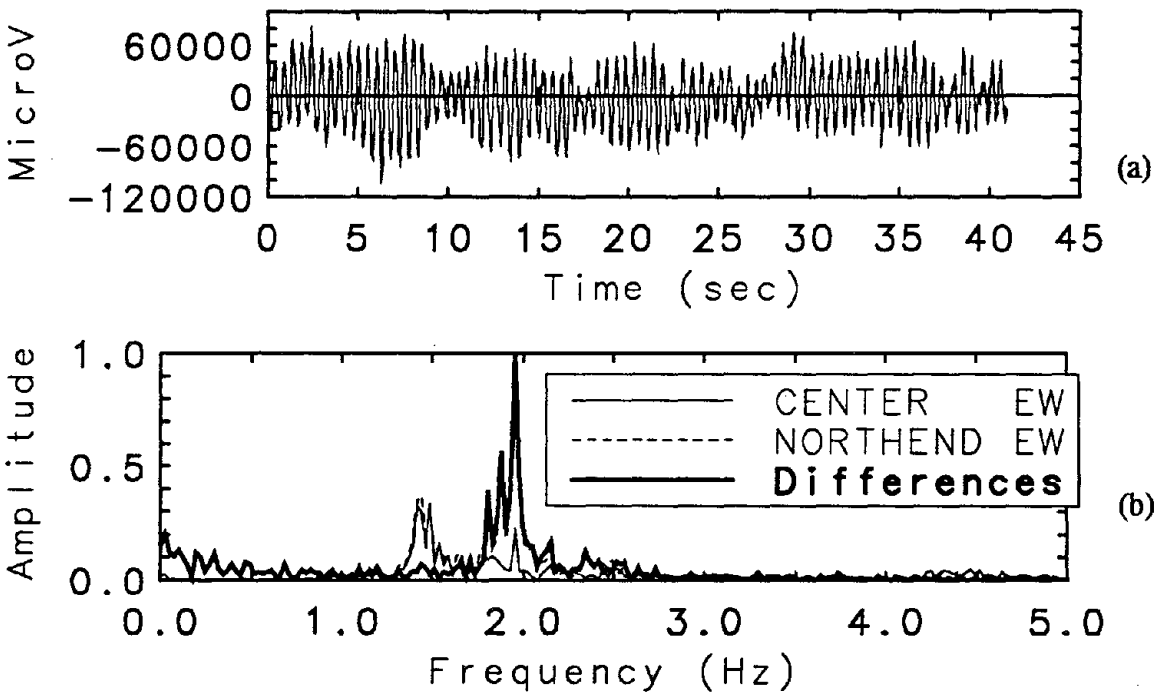

Figure 2.14 Difference of Roof-level EW Response to Ambient Vibration (a) and Corresponding Fourier Spectrum (b).

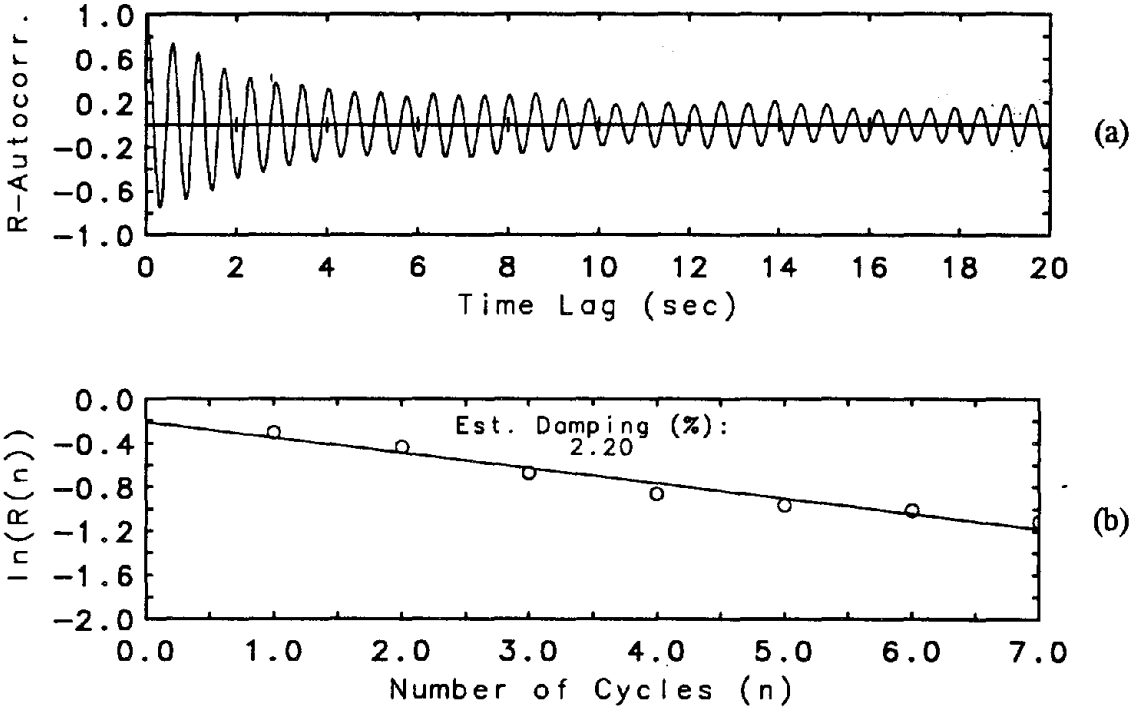

Figure 2.15 Autocorrelation of Ambient Vibration Response at Center of Roof in NS Direction (a) and Logarithmic Decrement for Damping Estimate (b).

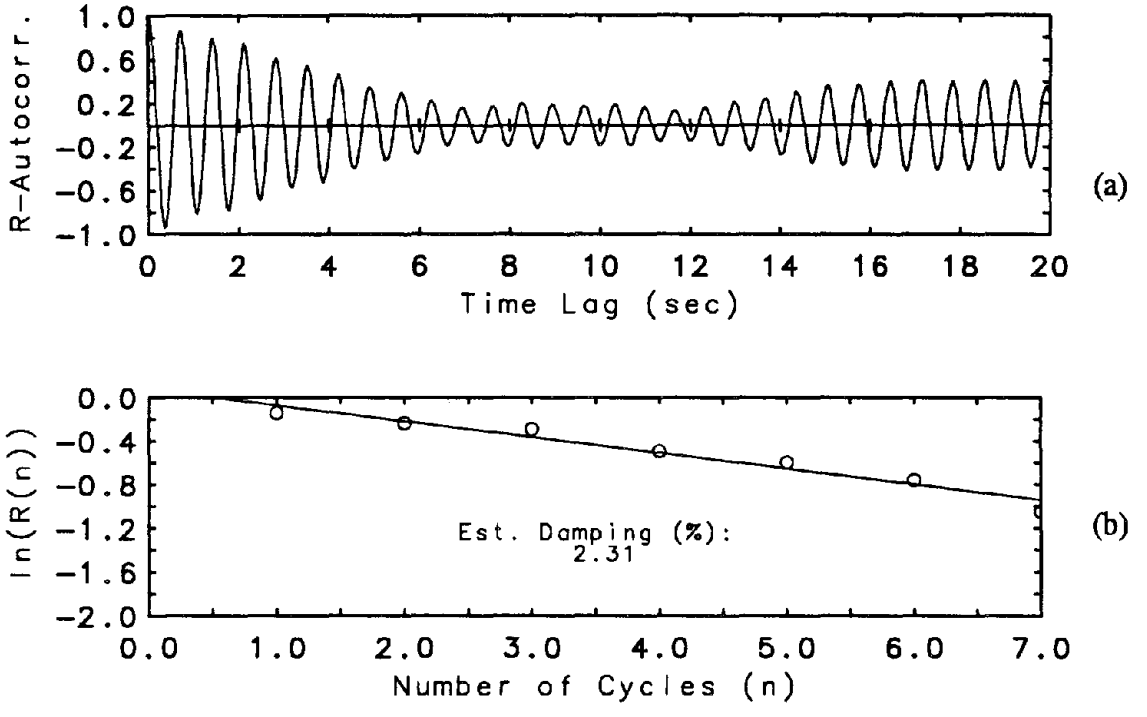

Figure 2.16 Autocorrelation of Ambient Vibration Response at Center of Roof in EW Direction (a) and Logarithmic Decrement for Damping Estimate (b).

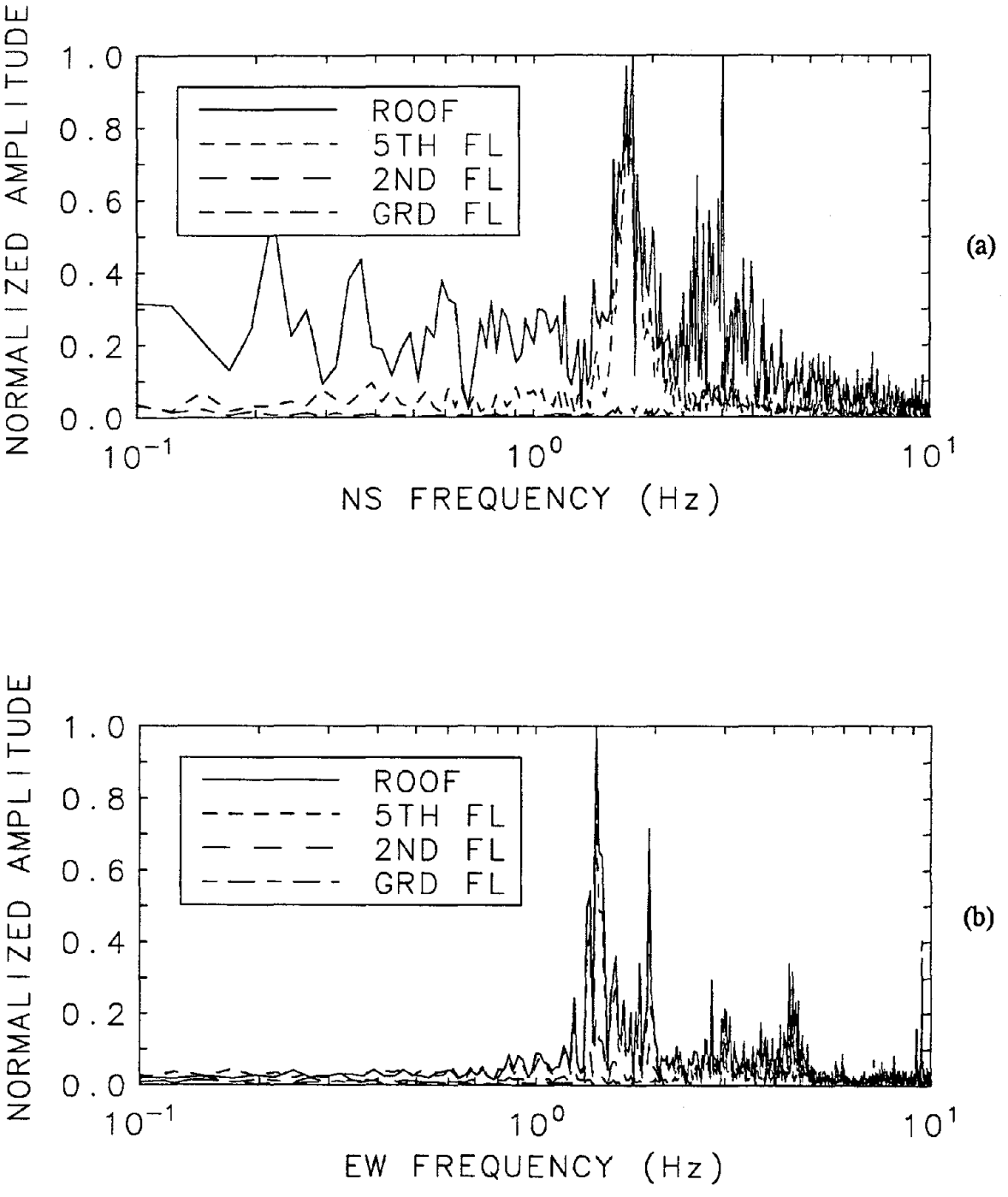

Figure 2.17 Normalized Fourier Spectra of Ambient Vibration Records at Different Elevations in NS (a) and EW (b) Directions, and First-Mode Response Mode Shape Due to Ambient Vibration (c).

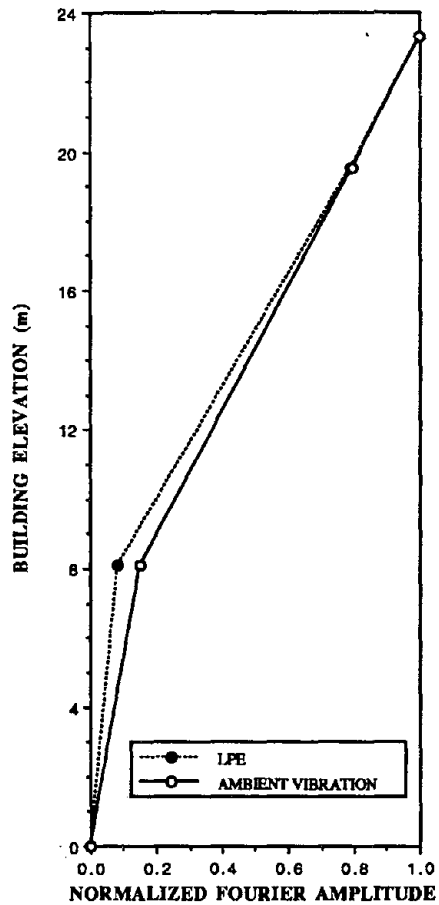

(c)

Figure 2.17 (continued)

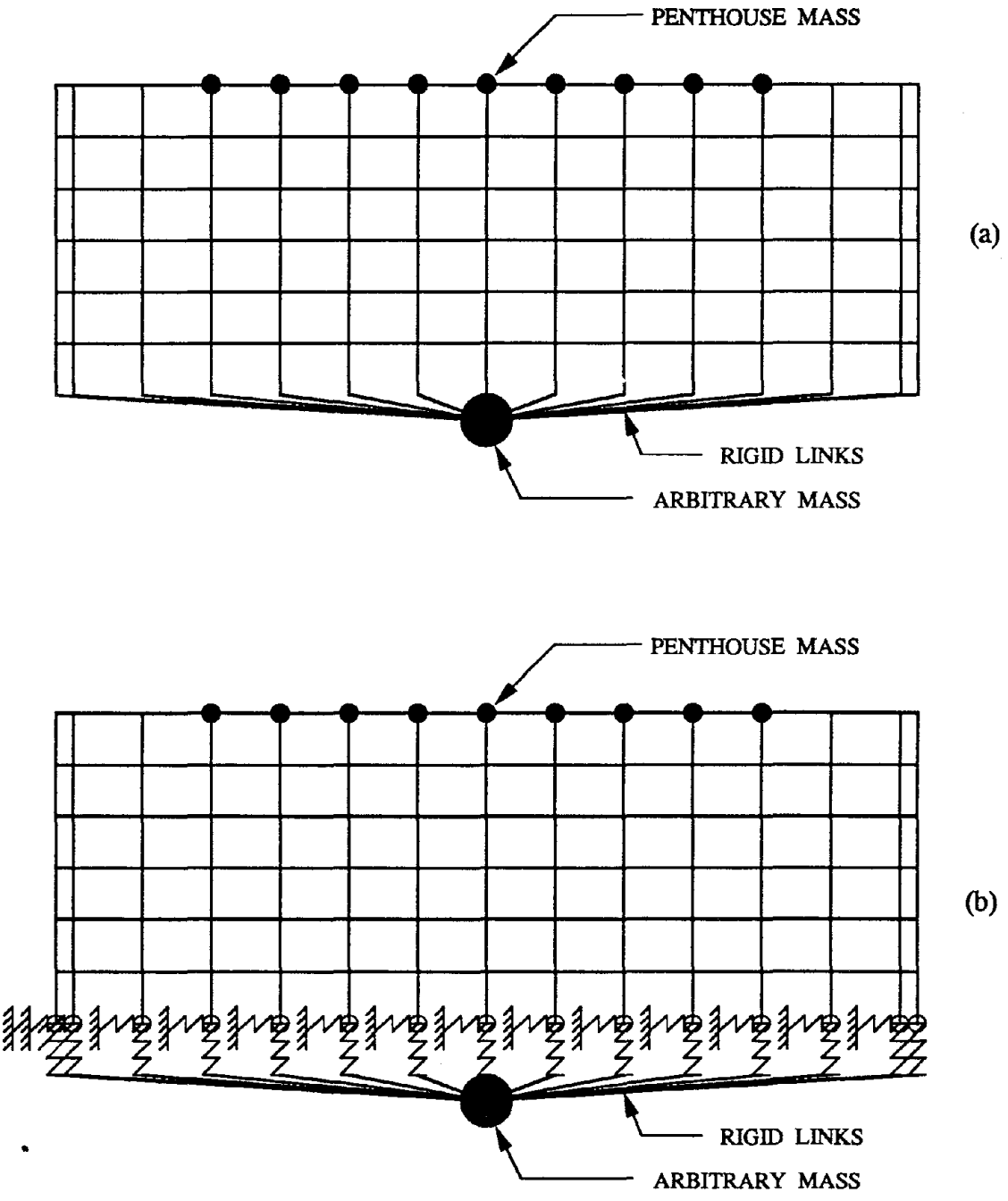

Figure 3.1 Finite Element Models of the San Bruno Commercial Office Building with Large Mass and Rigid Links, (a) Fixed-Base Model, and (b) Spring-Supported Model.

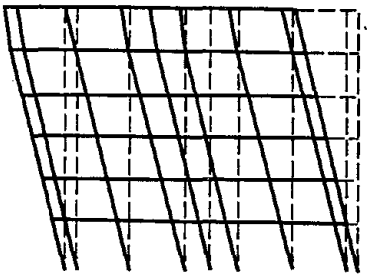

EW Translation

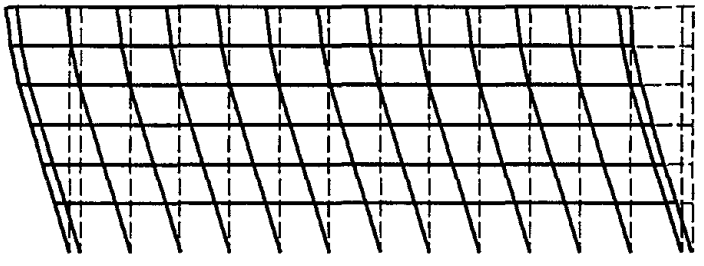

NS Translation

Figure 3.2 Mode Shape of the Fixed-Base Model.

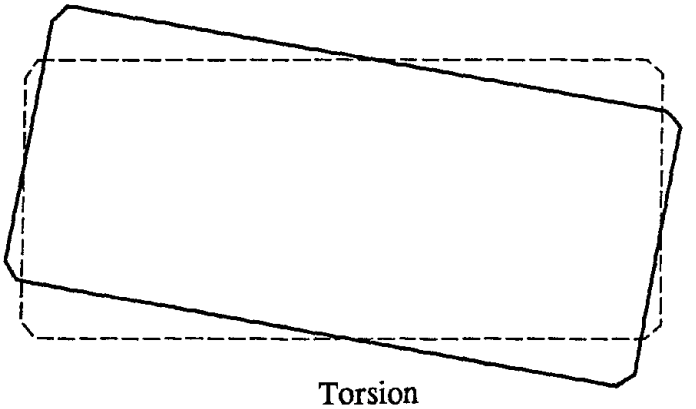

Torsion

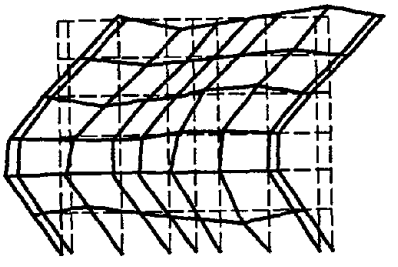

EW Translation with Floor Twisting

Figure 3.2 (continued)

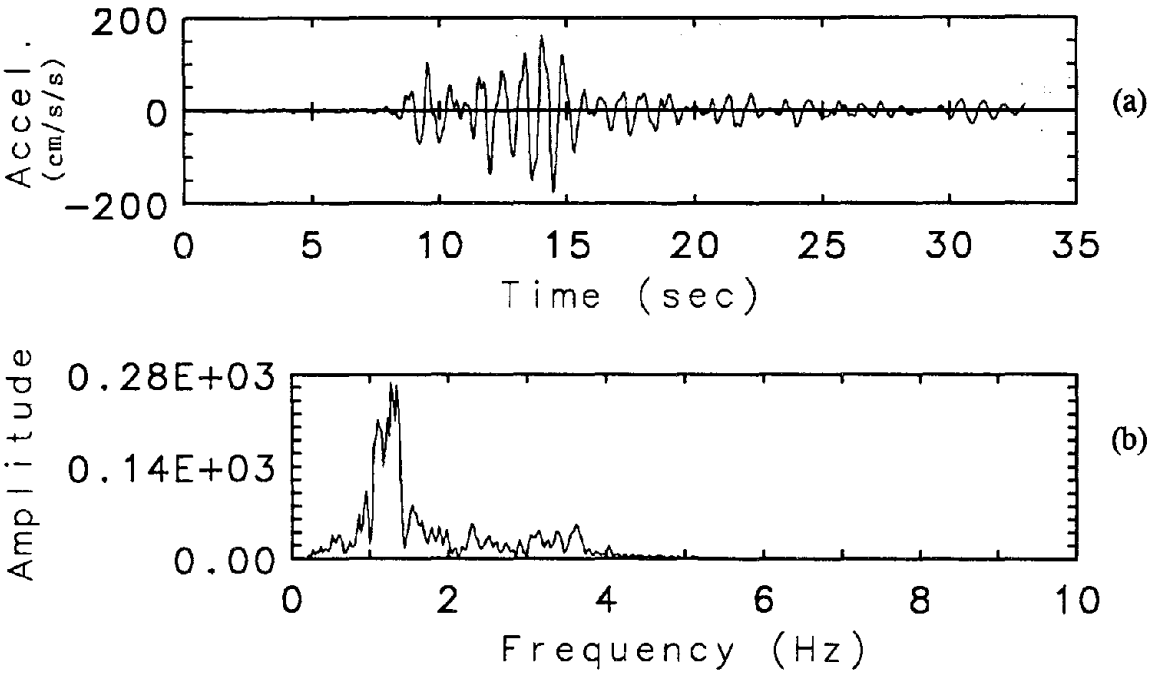

Figure 3.3 EW Acceleration-Time History at Center of Roof from the Fixed-Base Model with 10% Damping (a), and Corresponding Fourier Spectrum (b).

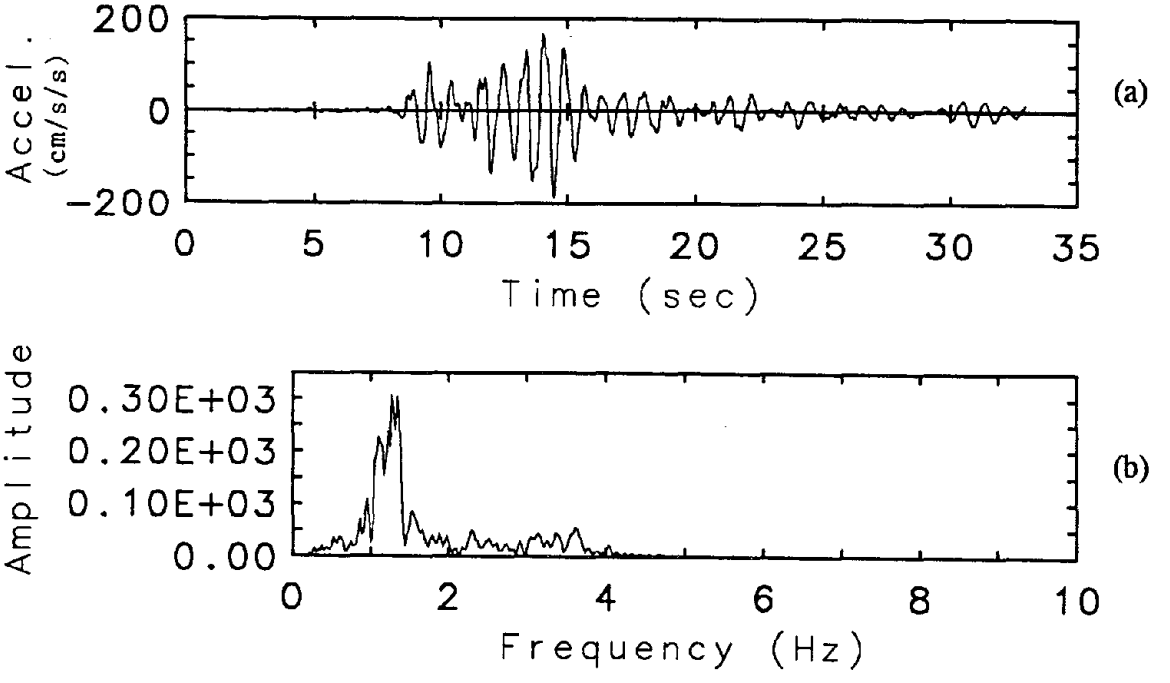

Figure 3.4 EW Acceleration-Time History at North End of Roof from the Fixed-Base Model with 10% Damping (a), and Corresponding Fourier Spectrum (b).

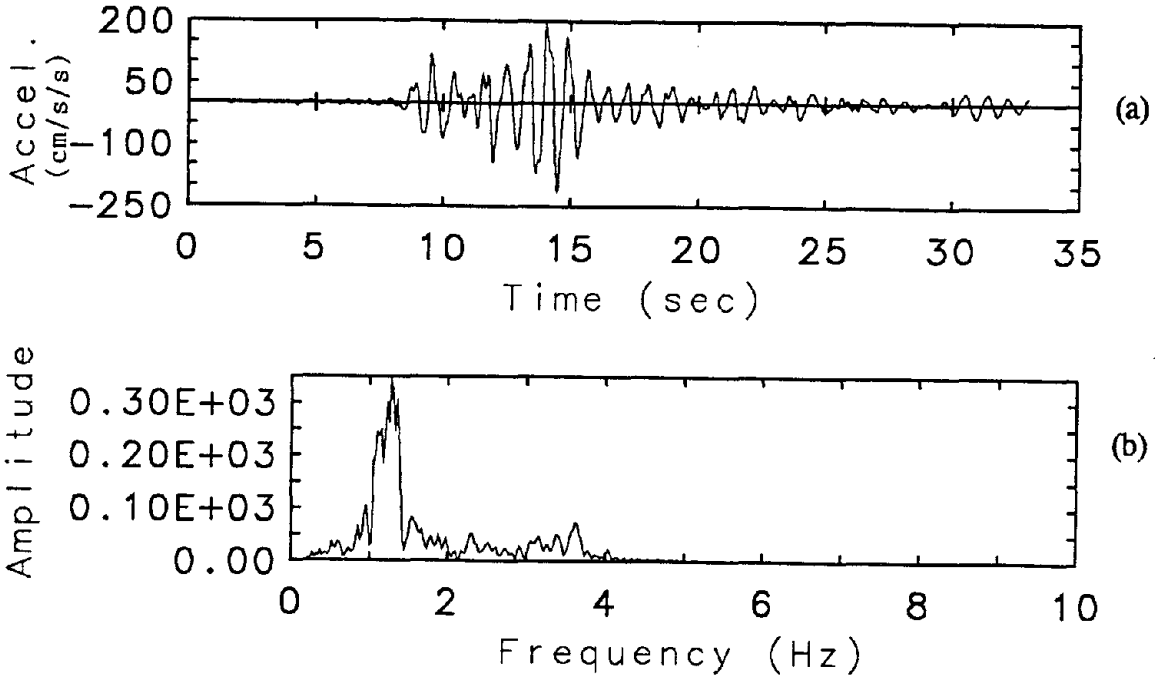

Figure 3.5 EW Acceleration-Time History at Center of Roof from the Fixed-Base Model with 7% Damping (a), and Corresponding Fourier Spectrum (b).

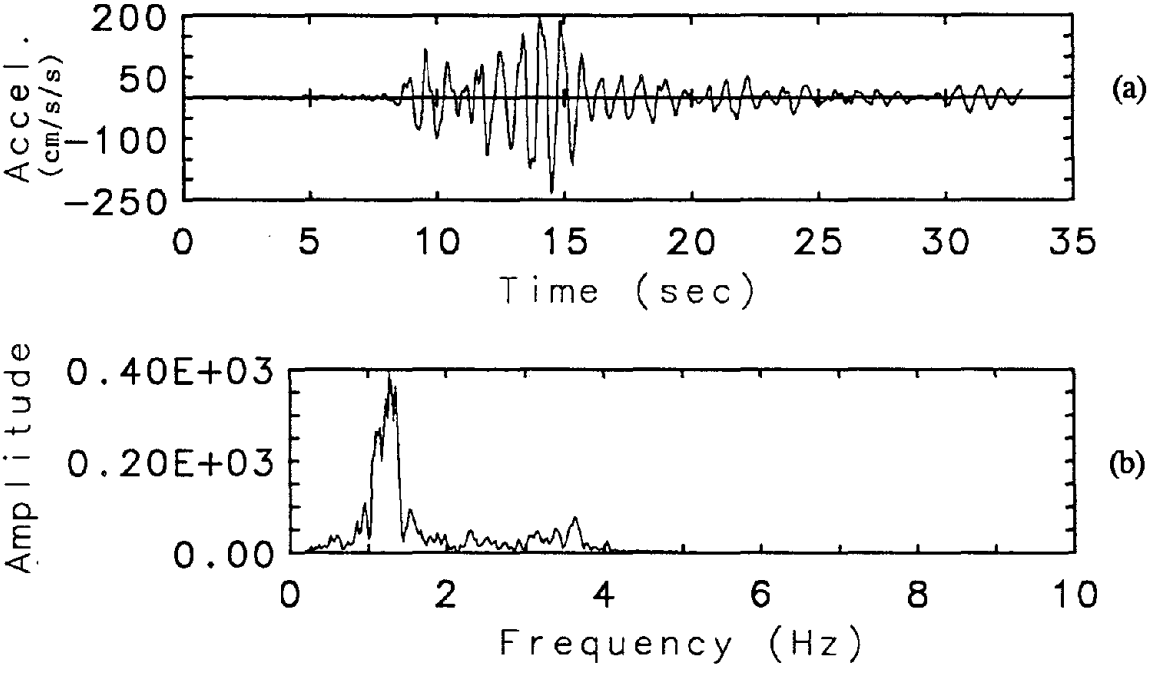

Figure 3.6 EW Acceleration-Time History at North End of Roof from the Fixed-Base Model with 7% Damping (a), and Corresponding Fourier Spectrum (b).

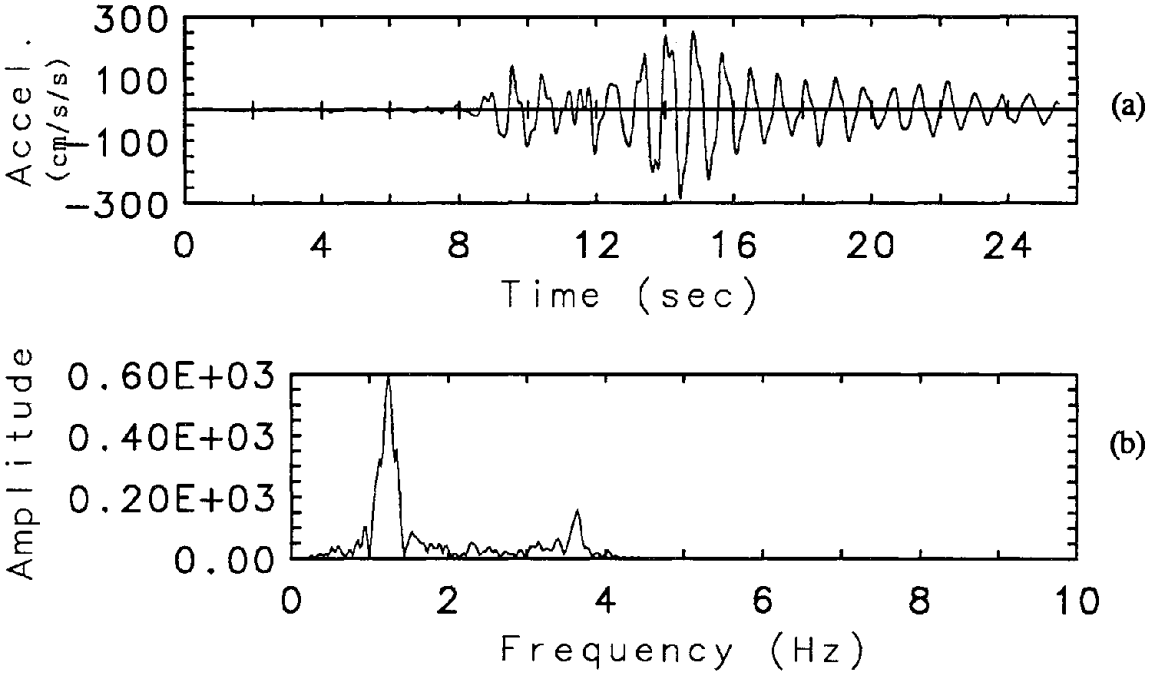

Figure 3.7 EW Acceleration-Time History at Center of Roof from the Fixed-Base Model with 3% Damping (a), and Corresponding Fourier Spectrum (b).

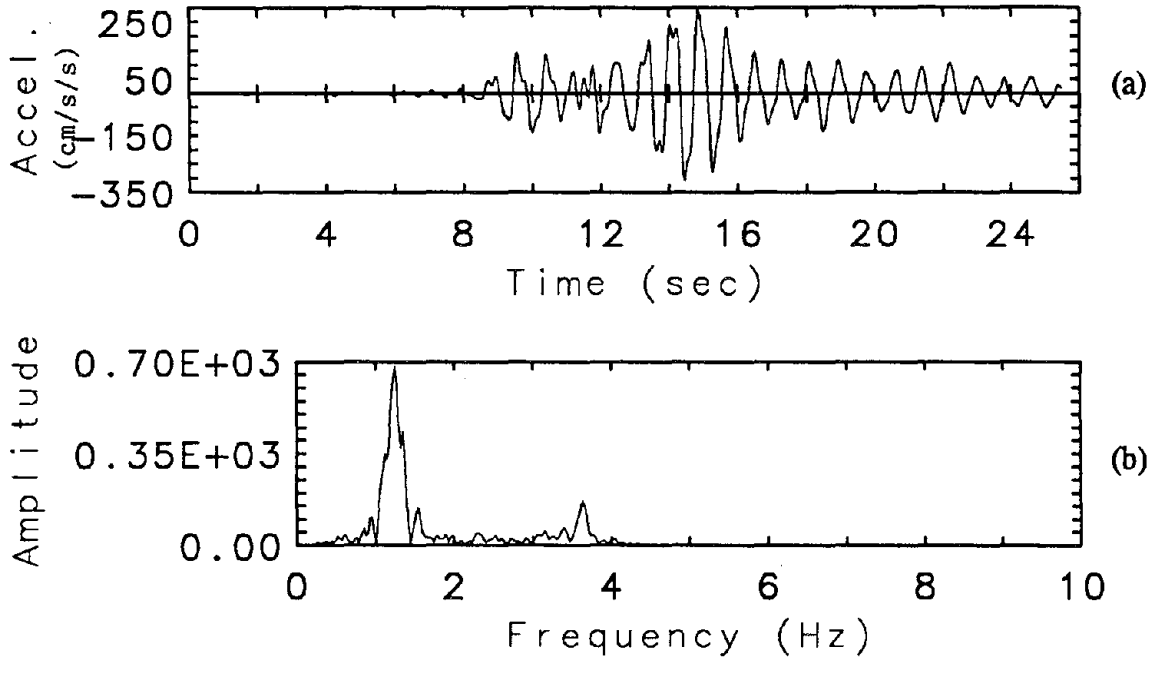

Figure 3.8 EW Acceleration-Time History at North End of Roof from the Fixed-Base Model with 3% Damping (a), and Corresponding Fourier Spectrum (b).

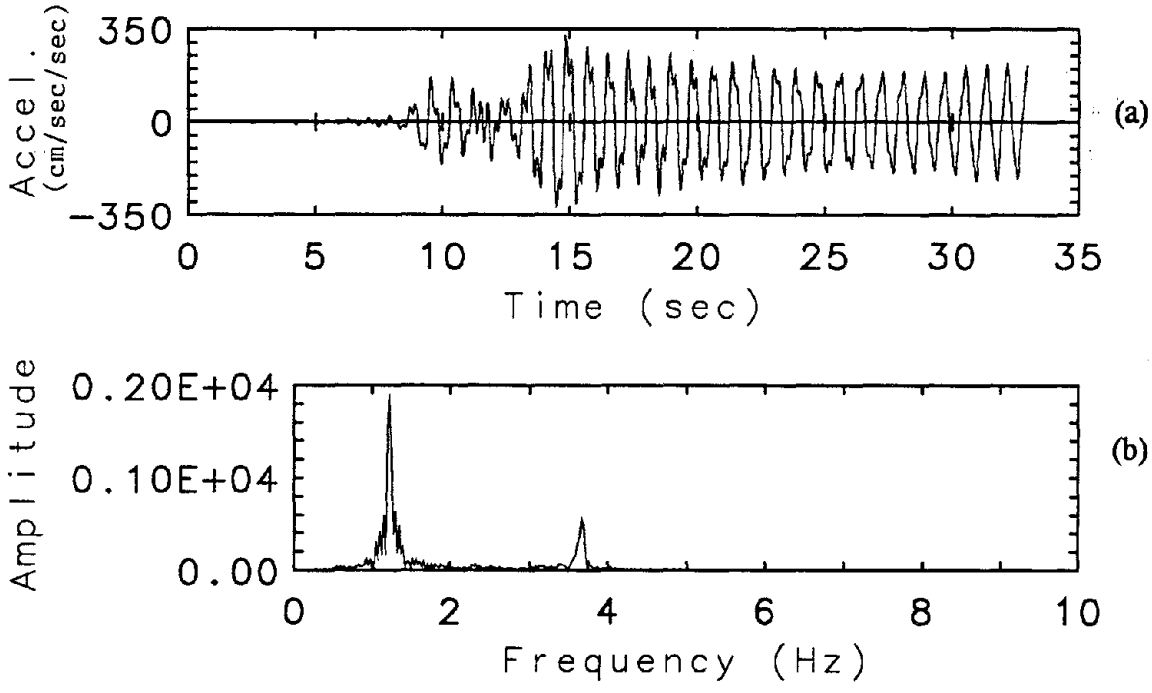

Figure 3.9 EW Acceleration-Time History at Center of Roof from the Fixed-Base Model with 0.5% Damping (a), and Corresponding Fourier Spectrum (b).

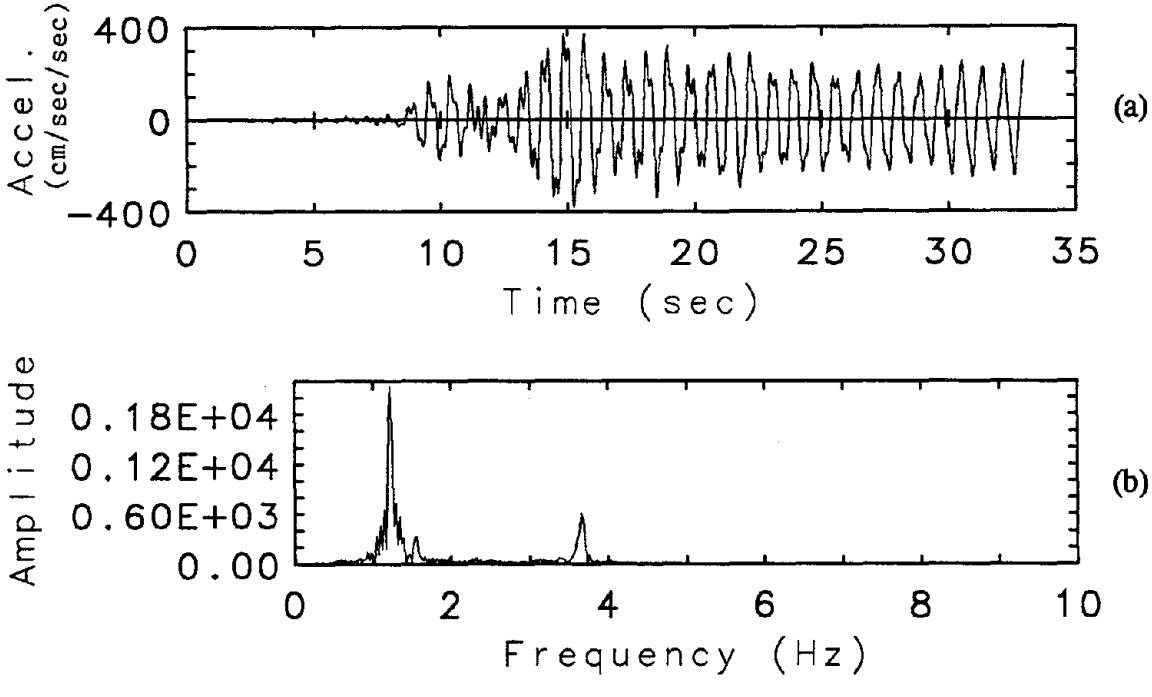

Figure 3.10 EW Acceleration-Time History at North End of Roof from the Fixed-Base Model with 0.5% Damping (a), and Corresponding Fourier Spectrum (b).

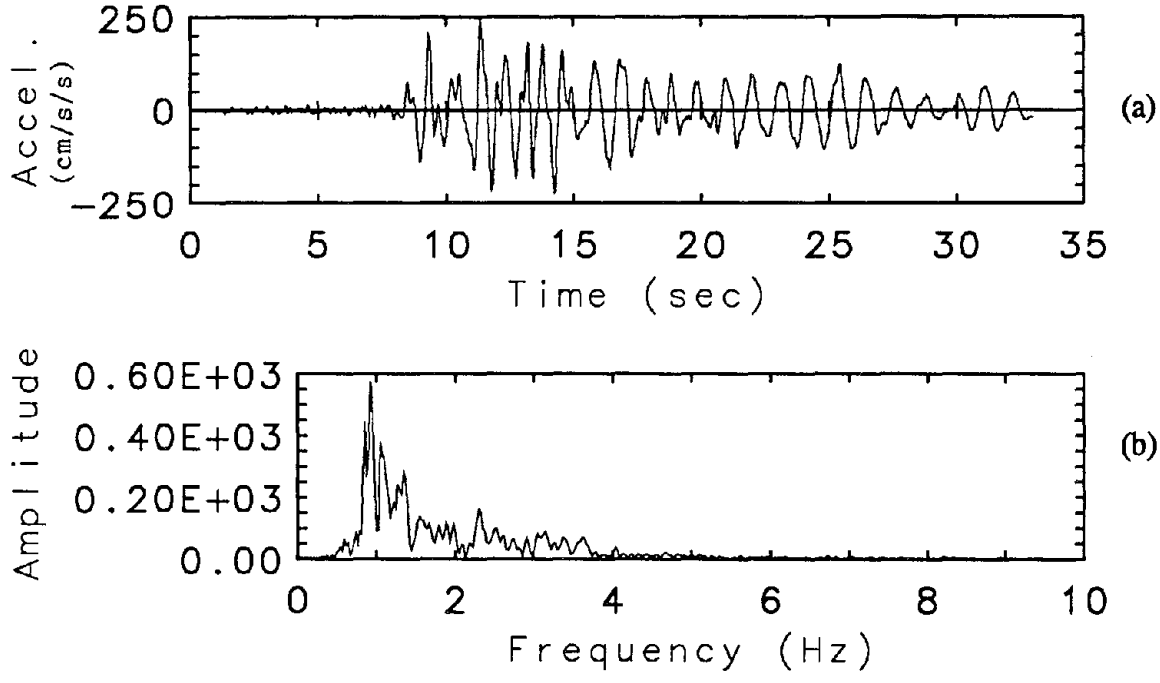

Figure 3.11 EW Acceleration-Time History of Center of Roof from the Spring-Supported Model with Rotational Spring Stiffness of 10^8 kN-m/rad (a), and Corresponding Fourier Spectrum (b).

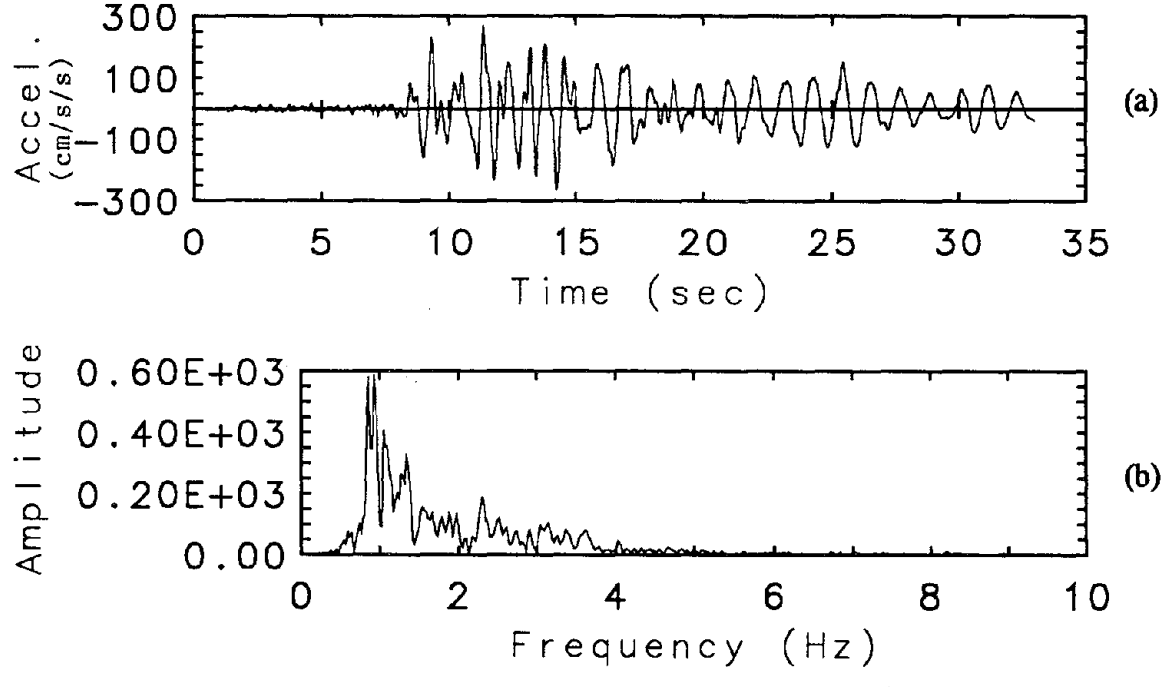

Figure 3.12 EW Acceleration-Time History of Center of Roof from the Spring-Supported Model with Rotational Spring Stiffness of 10^7 kN-m/rad (a), and Corresponding Fourier Spectrum (b).

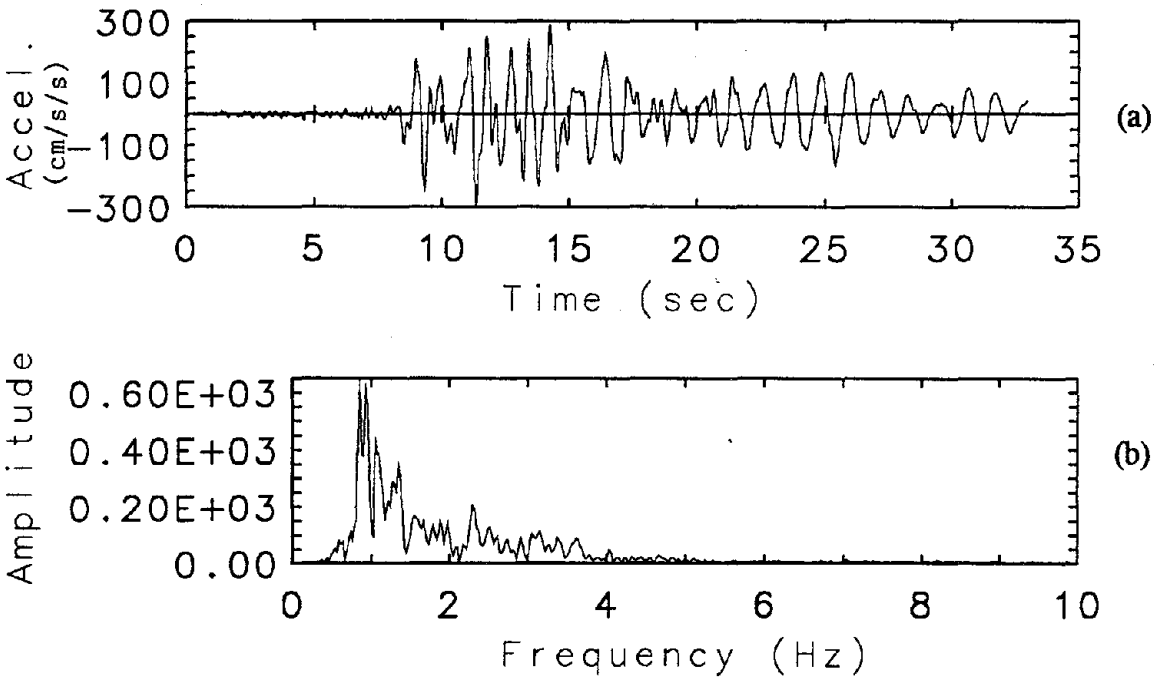

Figure 3.13 EW Acceleration-Time History of Center of Roof from the Spring-Supported Model with Rotational Spring Stiffness of 10^6 kN-m/rad (a), and Corresponding Fourier Spectrum (b).

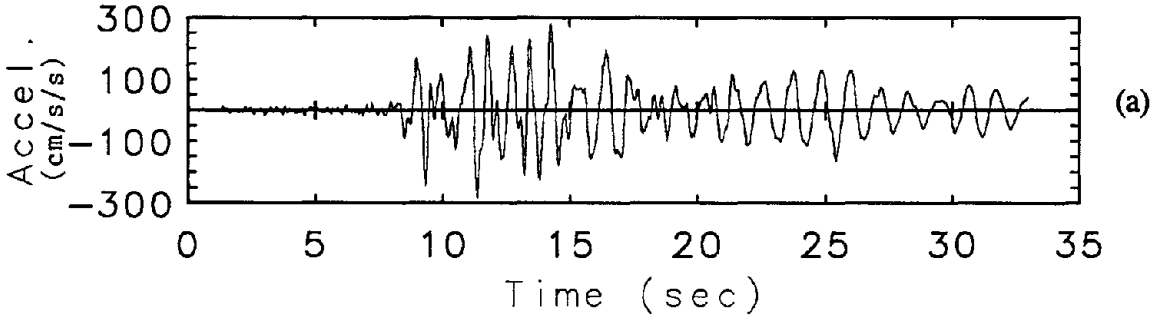

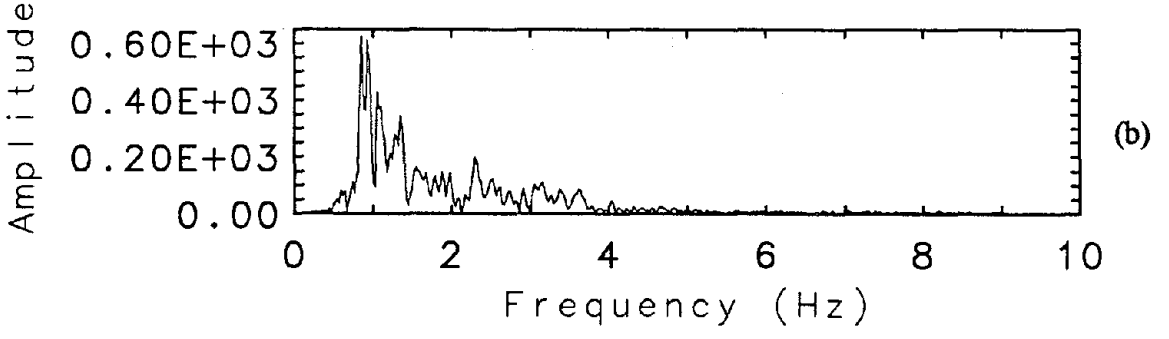

Figure 3.14 EW Acceleration-Time History of Center of Roof from the Spring-Supported Model with Rotational Spring Stiffness of 0.5×10^6 kN-m/rad (a), and Corresponding Fourier Spectrum (b).

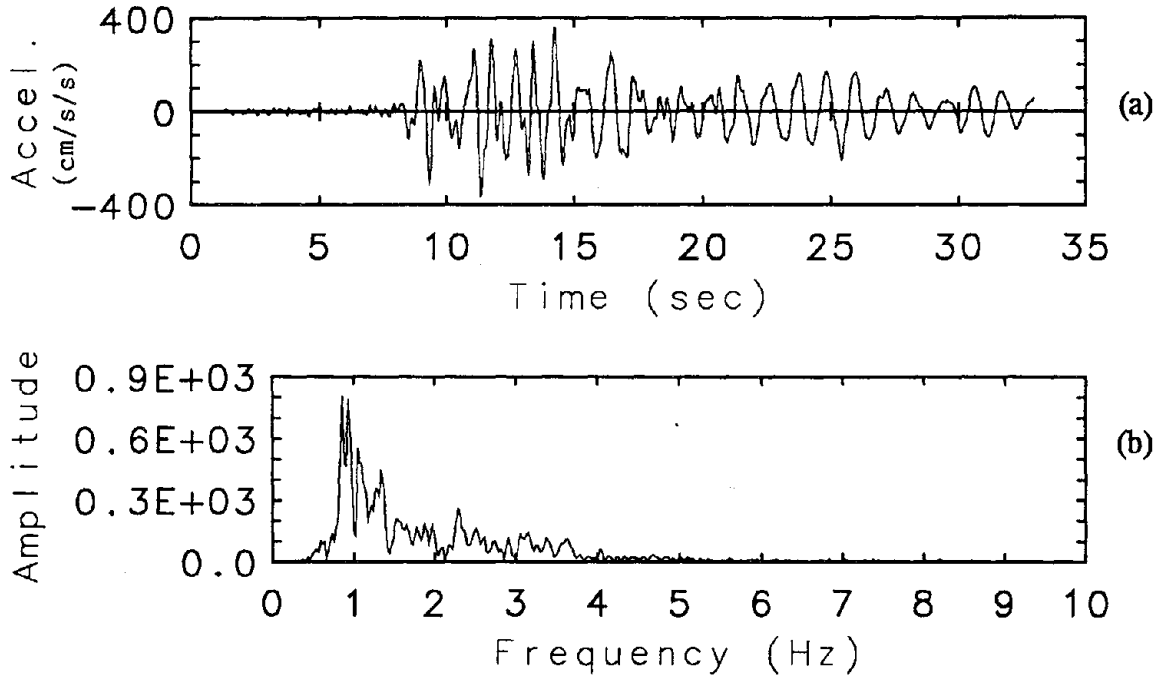

Figure 3.15 EW Acceleration-Time History of Center of Roof from the Spring-Supported Model with Rotational Spring Stiffness of 10^3 kN-m/rad (a), and Corresponding Fourier Spectrum (b).

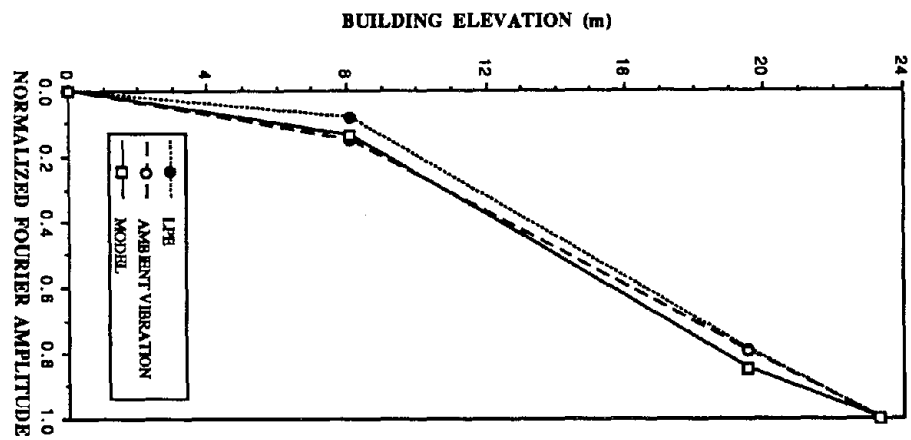

Figure 3.16 First-Mode Response Mode Shape Due to the LPE, Ambient Vibration, and the Spring-Supported Model.